

Learning Semiconductor Devices with MicroTec

Computer Aid for the book “Solid State Electronic Devices”
by Ben G. Streetman and Sanjay Banerjee

Siborg Systems Inc
Waterloo, Ontario N2L 5B1
Canada

Copyright ©2000 by Siborg Systems Inc.
All Rights Reserved.
First Printing August 2000.

Photocopying or any other reproduction of any part of this document violates copyright law.
Additional copies of this document are available from the publisher:

Siborg Systems Inc.
24 Combermere Cres.
Waterloo, Ontario
N2L 5B1
CANADA

Phone (519) 888-9906
FAX (519) 725-9522
E-mail microtec@siborg.ca
Web <http://www.siborg.ca>

Trademarks

MicroTec™, SiDif™, MergIC™, SemSim™, and SibGraf™ are trademarks of Siborg Systems Inc.

Microsoft, MS-DOS, Windows NT, Windows 95/98/2000 are registered trademarks of Microsoft Corporation

IBM is a registered trademark of International Business Machines Corporation.

Table of Contents

Introduction	5
MicroTec Environment	7
MicroTec Graphical User Interface	7
Problems	9
Problem 5.4	9
Problem 5.5	10
Problem 5.6	11
Problem 5.9	12
Problem 5.10	13
Problem 5.12	14
Problem 5.13	15
Problem 5.14	16
Problem 5.15	18
Problem 5.16	19
Problem 5.19	20
Problem 5.25	28
Small MicroTec Tutorial	31
Tech Stuff	31
Using MicroTec	31
Project selection/creation screen	31
SiDif	31
SemSim	31
MergIC	31
Batch Mode	31
Project settings and execution.	32
Directives	32
Subdirectives	32
Parameters	32
Viewing output	32
SibGraf Map	32
SibGraf 3D	32
SibGraf 2D	33
General Tips	33
Device Simulation Directives and Parameters	35

Run Requirements	35
Electrodes	35
IV Data	35
Doping wells	35
Tips	35
Batch mode	35
Doping wells	35
Axes	35
Output	36
Ramping	36
SibGraf 3D	36
SibGraf Map	36
SibGraf 2D	36
Electrodes	36
Building the p-n junction	37
Index	39
List of Figures	41

1. Introduction

This document contains solutions for selected numerical problems from the textbook “Solid State Electronic Devices” by Ben G. Streetman and Sanjay Banerjee. It is complemented by a visualization tool and a set of files containing information on the distributions of various device variables as well as their I-V characteristics.

The exercises are based on the use of MicroTec: 2D Semiconductor Process and Device Simulator. MicroTec is a widely recognized educational tool, now accepted by more than 80 universities in 25 countries including the University of California at Berkeley and Waseda University in Tokyo. The software enables students to create their own devices and test them under varying real world parameters. John Wiley & Sons have used the program as a supplement to a recently published book, [“Semiconductor Devices Explained: Using Active Simulation”](#) by Ton Mouthaan.

Despite its apparent simplicity, MicroTec is used by process engineers in more than 20 companies worldwide including Hitachi, NTT, General Electric, Cree Research and Rockwell Semiconductors.

Numerical simulation allows a more detailed demonstration of the physics underlying semiconductor devices. Essentially it enables to plot unlimited number of graphs complementing the textbook figures. The ease-of-use and flexibility of the graphical user interface allow to efficiently manipulate simulation results and plot various variables such as electrostatic potential, electric field, quasi-Fermi levels, current densities etc. It provides efficient means to learn device physics using a “what if” approach. This approach requires much less mathematical knowledge than the textbook and at the same time allows to qualitatively understand the underlying physics. It also gives an excellent realistic “feel of number” for various phenomena.

The numerical simulation examples are built as close as possible to the textbook problems. There are a number of models that are available in MicroTec. Some of them are more complicated, and conform with real world physics more closely than the textbook models. Therefore MicroTec can be used to widen the physical picture by adding realistic models and demonstrating “secondary effects”. For example, the conventional p-n junction theory used in the book does not take into account space charge of the mobile carriers, thus leaving out effects at the edges of the space charge region, like the spill-over effect and high level injection. MicroTec on the other hand, allows one to analyze these effects and to show when they become important.

It is arguable that a course without analytical expressions for device analysis may not be widely accepted but it may definitely be used in some instances. For example, process engineers, the primary users of MicroTec in semiconductor industry, do not need to know much about analytical models but need to understand what happens, say, if the implant dose is changed by 10 KeV. In this case MicroTec is a very powerful tool to have. Ultimately it may be used as a “virtual fab” to analyze semiconductor processes and to teach process engineers the device physics.

2. MicroTec Environment

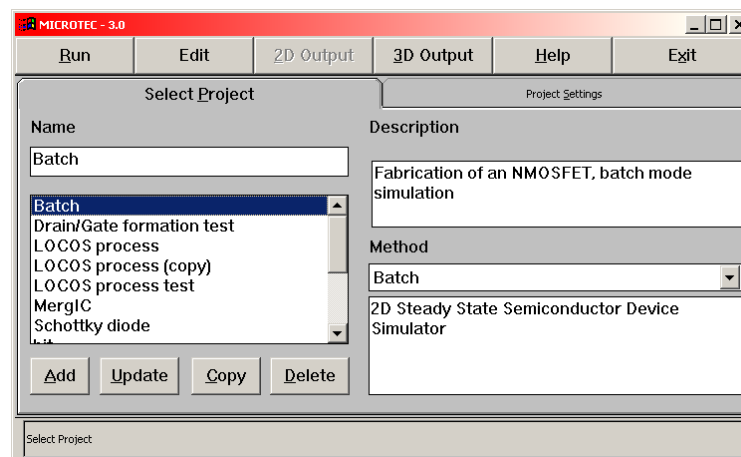
MicroTec is a shell integrating a few programs for semiconductor process and device simulation. [SiDif](#) is a two dimensional simulator for implantation, epitaxy, diffusion and oxidation, [SemSim](#) is a two dimensional steady-state SEMiconductor device SIMulator and SibGraf is an interactive 3D and 2D graphing program.

The true power of MicroTec is felt when SiDif and SemSim are used together in a virtual fab manner: simulate fabrication of the device structure first and then simulate the device characteristics. However, following the textbook exercises, we will run SiDif and SemSim independently, and use SibGraf to show the results.

This package includes only the graphical user interface of MicroTec. You will be able to generate all the graphs presented below as well as a vast variety of additional curves, surfaces and variables. You also will be able to explore how the input data are modified and new devices are created. However it will not be possible to simulate the newly defined fabrication processes or devices because the simulators themselves are not included in the package. All the data for the textbook exercises have been calculated in advance and are included in the package.

2.1 MicroTec Graphical User Interface

To invoke MicroTec, unzip the attached archive in any directory and run MicroTec.exe. The following window will pop-up:



To manipulate the data, select a project in the project list window on the [Select Project](#) page by clicking the left mouse button on the project name.

MicroTec has a choice of three visualization modes: 2D, 3D or colour map/contour.

- ▶ To plot I-V curves the [2D Output](#) button is used. Curves may be added to the graph by using Plot/Add menu. Select X and Y columns to be used as X and Y axis data on the plot and click Add and then Okay.
- ▶ Two-dimensional distributions of doping concentration, electrostatic potential etc may be plotted using the [3D Output](#) button. The 3D Output button takes the user to a colour map view of the electrostatic potential distribution in a device. Other variables may be chosen from the Plot/

MicroTec Environment

Select menu. In the colour map view, the fourth button from the right will open a new window with a 3D surface representation of the same data.

To modify project settings, select a project and click on the **Project Settings** tab. Another page of the main MicroTec window will appear showing an editable list of directives, subdirectives and parameters. Click on a folder symbol to open it. Double-click a parameter to edit it. If you click on any item with the left and then the right mouse button, a new window pops up with a menu allowing you to delete, copy, add or insert a directive, subdirective or parameter.

A more detailed description of MicroTec is given below in the "**Small Tutorial**", included in this package or in the **Manual** available at the Web Site <http://www.siborg.ca>.

3. Problems

The following problems are from chapter 5 in the book.

3.1 Problem 5.4

We wish to do an As implant into a Si wafer with a 0.1 μm oxide such that the peak lies at the oxide silicon interface, with a peak value of $5 \times 10^{19} \text{ cm}^{-3}$. What implant parameters (energy, dose and beam current) would you choose? The scan area is 200 cm^2 , and the desired implant time is

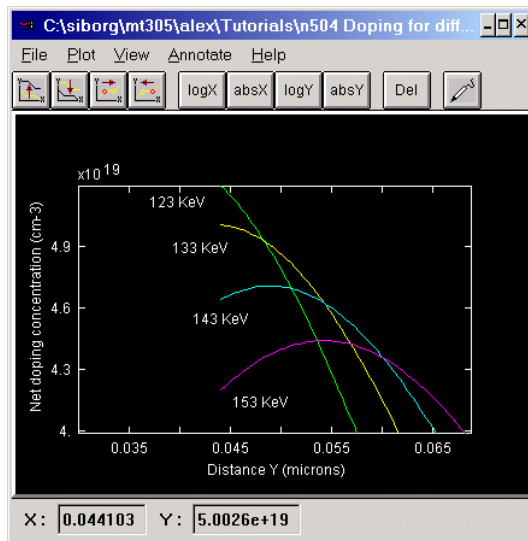


Figure 5.4.1 Arsenic concentration profiles at different implant energies.

Yellow project a, green project b, cyan project c, magenta project d. Graph has been zoomed.

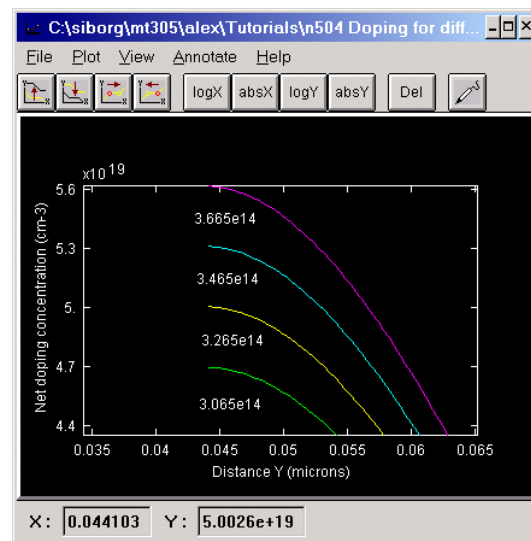


Figure 5.4.2 Arsenic concentration profiles at different implant doses.

Yellow project a, magenta project g, cyan project f, green project g. Graph has been zoomed.

20 s. Assume similar range statistics in oxide and Si.

Projects a-g

The projects 5.4a-g all have similar geometry, models and process steps, and differ by Arsenic implant energies and doses. The domain was made to be $1 \times 1 \mu\text{m}$, with 5 and 1000 nodes in the X and Y directions respectively. The original undoped substrate orientation was set to $\langle 100 \rangle$. Wet oxidation was done at 1000°C for 245 s, yielding a $0.1 \mu\text{m}$ oxide layer. Blanket arsenic implant at different doses and energies was applied.

Solution

During wet oxidation, H_2O is flowed over Si at atmospheric pressure at some high temperature. In the process, Si is consumed from the surface. For each $1 \mu\text{m}$ of SiO_2 grown, $0.44 \mu\text{m}$ of Si is consumed. For the yellow curve the projected range may seem to be only $\sim 0.044 \mu\text{m}$, but this number must be divided by 0.44 to get the true interface depth of $0.1 \mu\text{m}$. This seeming peculiarity is caused because MicroTec does not show the oxide which is above the original Si surface. Although the oxide above the surface is taken into account when calculating implantation pro-

Problems

files, only the oxide inside the silicon is displayed. An energy of 133 KeV and a dose of $3.265 \times 10^{14} \text{ cm}^{-2}$ were used to obtain the desired implant depth of $0.1 \text{ }\mu\text{m}$ and concentration of $5 \times 10^{19} \text{ cm}^{-3}$. From the graph 5.4.1 it may be noted that an increase in implant energy causes the maximum concentration of an implant to shift deeper into the Si and increases the straggle which in turn causes the maximum concentration to decrease. Because of the zoom, it is not instantly apparent that the distributions seen in the figures are in fact gaussian.

From figure 5.4.2 we see a direct relationship between the Arsenic implant dose and the concentration at the oxide-silicon interface.

It is now a straight forward task to calculate the beam current, which is calculated from $(q \cdot \text{area} \cdot \text{dose}) / \text{time} = (1.6 \times 10^{-19} \text{ C}) \cdot (200 \text{ cm}^2) \cdot (3.57 \times 10^{14} \text{ cm}^{-2}) / (20 \text{ s}) = 5.7 \times 10^{-4} \text{ A}$.

3.2 Problem 5.5

We want to implant $5 \times 10^{14} \text{ cm}^{-2}$ B into Si at an average depth of $0.5 \text{ }\mu\text{m}$. We have an implanter which has a maximum acceleration voltage of 150 kV. How can we achieve this profile if we have singly and doubly charged B in the machine? Suppose the doubly ionized beam current is 0.1 mA, how long will the implant take if the scan area is 100 cm^2 ? By doing clever ion implanter source design, Dr. Boron Maximus has increased the beam current by a factor of 1000. From a dose uniformity point of view is this good or bad?

Project

The domain was made to be $1 \times 1 \text{ }\mu\text{m}$, with 5 and 200 nodes in the X and Y directions respectively. The original undoped substrate orientation was set to $\langle 100 \rangle$. Blanket boron implant at different doses and energies was applied until the proper profile was achieved.

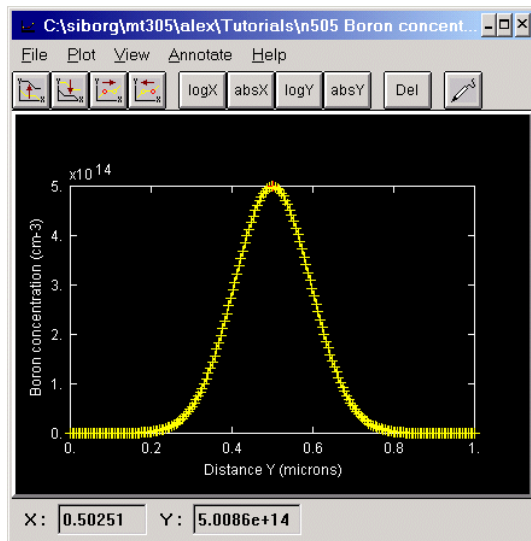


Figure 5.5.1 Boron concentration profile. Implant dose is $1.1823 \times 10^{10} \text{ cm}^{-2}$ and implant energy is 192 KeV.

Solution

Let us assume that we are able to separate the doubly ionized boron from the singly ionized boron with the use of a magnetic separator. As a result, only the doubly ionized boron will enter the implanter drift tube and so reach the silicon. Since the maximum acceleration voltage of the implanter is 150 kV, for doubly ionized B it will be equivalent to a maximum of 300 kV.

To achieve the desired concentration and depth, implant dose of $1.1823 \times 10^{10} \text{ cm}^{-2}$ and implant energy of 192 KeV were used. Figure 5.5.1 shows the concentration profile that was obtained. The gaussian distribution is clearly visible.

We may calculate the time of the implant from the equation used in question 5.4, only now the current is known and we are looking for t:

$t = (2 * q * \text{area} * \text{dose}) / \text{current}$. q is multiplied by 2 because only doubly charged boron hits the silicon.

$$t = (2 * 1.6 \times 10^{-19} \text{ C} * 100 \text{ cm}^2 * 1.1823 \times 10^{10} \text{ cm}^{-2}) / (0.1 \times 10^{-3} \text{ A}) = 3.8 \times 10^{-3} \text{ s}$$

Increasing current by a factor of 1000 will result in fewer scans being performed in order to reach the desired concentration. Making fewer scans means that uniformity will suffer.

For details concerning the effects of different implant energies and doses, see “Problem 5.4” on page 9

3.3 Problem 5.6

Assuming a constant (unlimited) source diffusion of P at 1000 °C into p-type Si ($N_a = 2 \times 10^{16} \text{ cm}^{-3}$), calculate the time required to achieve a junction depth of 1 micron.

Projects a-j

The projects 5.6a-j all have similar geometry, models and process steps, and differ by phosphor surface concentration, annealing times and temperatures. The domain was made to be $1 \times 2 \text{ }\mu\text{m}$, with 20 and 300 nodes in the X and Y directions respectively. The original substrate orientation was set to $\langle 100 \rangle$, with an initial boron concentration set to $2 \times 10^{16} \text{ cm}^{-3}$. Blanket phosphor deposition resulting in various surface concentrations was performed. Annealing was performed at 1000 °C for different lengths of time.

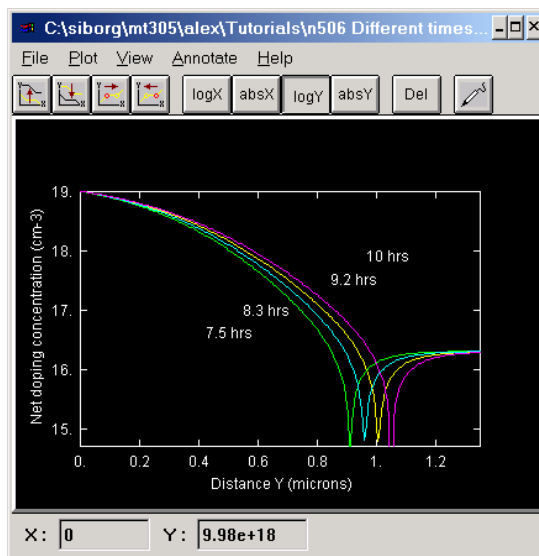


Figure 5.6.1 Logarithm of net doping concentration for different annealing times. Yellow project a, green project b, cyan project c, magenta project d. Graph has been zoomed.

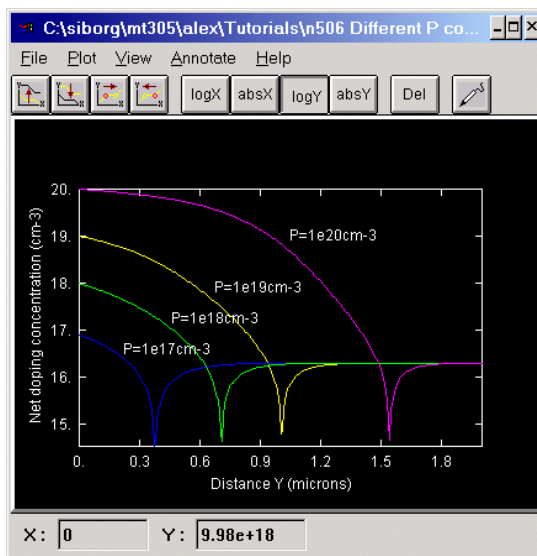


Figure 5.6.2 Logarithm of net doping concentration for different P surface concentrations. Yellow project a, blue project e, green project f, magenta project g.

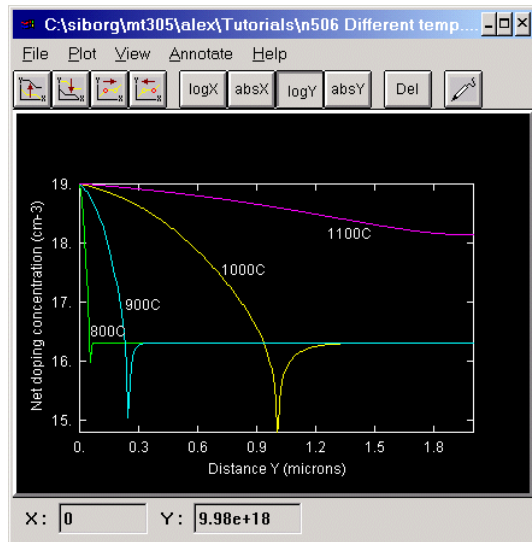


Figure 5.6.3 Logarithm of net doping concentration for different annealing temperatures. Yellow project a, cyan project i, green project h, magenta project j.

to a deeper junction as well as significantly heavier doping throughout the n-type side.

Figure 5.6.3 shows the effect of annealing temperature on junction depth. An exponential Arrhenius dependence of the diffusion coefficient is suggested in the figure. Higher temperature leads to a deeper junction.

3.4 Problem 5.9

An abrupt Si p-n junction has $N_a=10^{18} \text{ cm}^{-3}$ on one side and $N_d=5 \times 10^{15} \text{ cm}^{-3}$ on the other. a) Calculate the Fermi level positions at 300 K in the p and n regions. b) Draw an equilibrium band diagram for the junction and determine the contact potential V_0 from the diagram. c) Compare the results of part b with V_0 as calculated from Eq(5-8).

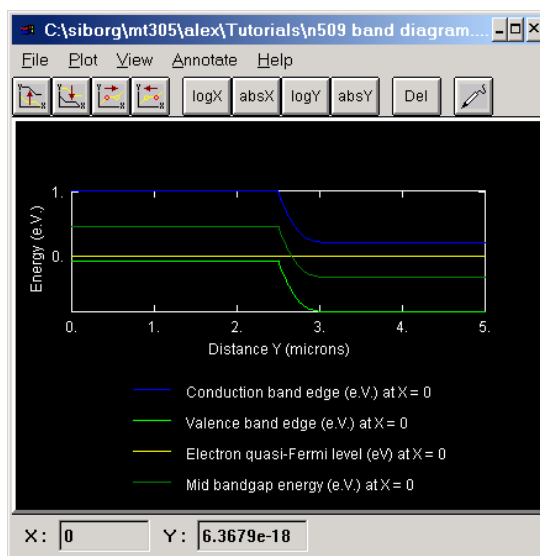


Figure 5.9.1 Electrostatic and Fermi potential.

Solution

Had the source of P been limited, a gaussian distribution would have been achieved, but in this diffusion the source was unlimited, and so the obtained distribution is called a complementary error function. The logarithmic scale is mandatory to see the p-n junction more clearly. The junction occurs where the introduced donor concentration just equals the substrate doping. With an initial phosphorus surface concentration of 10^{19} cm^{-3} and at $1000 \text{ }^\circ\text{C}$, the annealing time required for a $1 \text{ }\mu\text{m}$ junction depth was 9.2 hours. Figure 5.6.1 demonstrates the effects of annealing time on junction depth. Increased time leads to a deeper junction as well as heavier doping throughout the n-type side.

Figure 5.6.2 shows the effects of different initial phosphorus surface concentrations. The annealing time was fixed at 9.2 hrs. Increased surface concentration leads

Project

The X and Y domains were arbitrarily set to 5 and 5 μm . The p-side extends in the Y direction from 0 to 2.5 and the n-side from 2.5 to 5 μm with an abrupt junction. The number of nodes used in the X and Y direction were 5 and 100 respectively. No high doping, nor impact ionization effects were included. Default models for mobility, lifetime and bandgap were used. Two electrodes were specified at the top

and bottom of the domain. Only one IV point was calculated at 0 V bias.

Solution

At 0 V bias the electron and hole quasi-Fermi levels coincide with the Fermi level, which is constant and equal to 0 V throughout the p and n regions.

V_0 can be seen to be $\sim 0.330 \text{ V} + \sim 0.467 \text{ V} = \sim 0.797 \text{ V}$. The calculated contact potential V_0 according to Eq(5.8), was found to be $\sim 0.799 \text{ V}$.

3.5 Problem 5.10

The junction described in Prob. 5.9 has a circular cross section with diameter of $10 \mu\text{m}$. Calculate x_{n0} , x_{p0} , Q_{+} , and E_0 for this junction at equilibrium (300 K). Sketch $E(x)$ and charge density to scale, as in Fig. 5-12.

Projects a-c

The projects 5.10a-c all have similar geometry and models, and differ by doping levels. The X and Z domains were both set to $8.86 \mu\text{m}$, the Y domain to $3 \mu\text{m}$. Although the junction described in the question is cylindrical, the one we model is virtually 1D. This may be done because the junction width is small compared with the diameter of the device. The p-side extends in the Y direction from 0 to 0.5 and the n-side from 0.5 to $3 \mu\text{m}$ with an abrupt junction. The number of nodes used in the X and Y direction were 5 and 100 respectively. No high doping, nor impact ionization effects were included. Default models for mobility, lifetime and bandgap were used. Two electrodes were specified, one at the top and bottom of the domain. Only one IV point was calculated at 0 V bias.

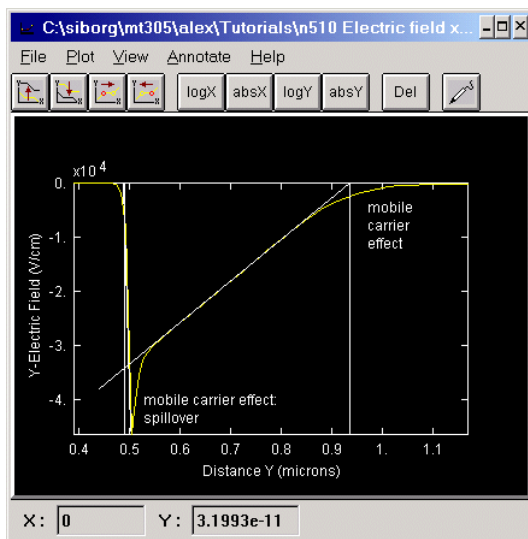


Figure 5.10.1 Electric field. Annotation lines mark the relative locations of x_{n0} and x_{p0} . Mobile carrier effects are clearly visible. Project a. Graph was zoomed.

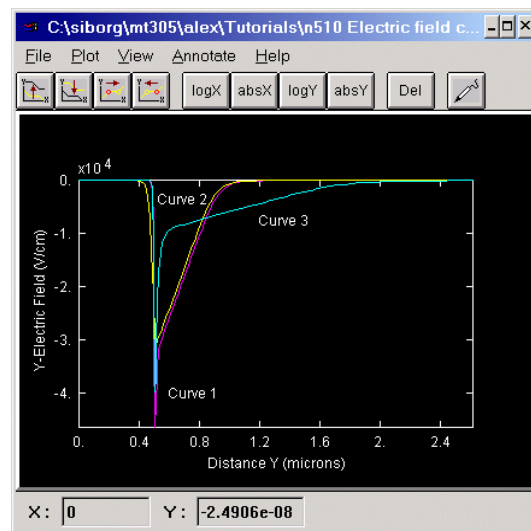


Figure 5.10.2 The effects of doping on peak electric field and spillover. Magenta project a, yellow project b, cyan project c. Graph was zoomed.

Solution

The calculated x_{n0} and x_{p0} were $0.45 \mu\text{m}$ and $0.002 \mu\text{m}$ respectively. These values compare well with the observed values of $x_{n0} = 0.44 \mu\text{m}$ and $x_{p0} = 0.007 \mu\text{m}$ (taking 0.5 as origin). The edges of the transition region have been drawn onto the graph (the material is p-type to the left of the junction, and is n-type to the right).

The calculated peak electric field is -34834 V/cm , while the observed is -34052 V/cm .

In unequally doped junctions, the depletion region extends further into the lighter doped side (to the right, in the figure). The sharp peak in the electric field (figure 5.10.1, and Curve 1 in figure 5.10.2) is caused by the spillover effect; holes from highly doped p-side ($N_a = 1 \times 10^{18} \text{ cm}^{-3}$) diffuse (spill) into n-type ($N_d = 5 \times 10^{15} \text{ cm}^{-3}$) material. Spillover is a result of the mobile carrier effect. Another result of the mobile carrier effect is the spreading out of the electric field at the space charge region edges. These phenomena are not taken into account by the simplified equations used in the textbook which do not include the contribution of the carriers ($p - n$) to the space charge. Therefore, in order to coincide with the results obtained in the book it is necessary to extrapolate the electric field plots like it is done in figure 5.10.1.

By diminishing the acceptor doping (now $N_a = 10^{17} \text{ cm}^{-3}$) we are able to reduce the spillover in figure 5.10.2 Curve 2, and not affect the extrapolated E_0 . Curve 3 shows the result of reducing the doping of the lighter doped side. Even a slight reduction in doping (now $N_d = 5 \times 10^{14} \text{ cm}^{-3}$ and $N_a = 10^{18} \text{ cm}^{-3}$) causes a noticeable decrease in E_0 .

3.6 Problem 5.12

A Si $p^+ - n$ junction has a donor doping of $5 \times 10^{16} \text{ cm}^{-3}$ on the n side and a cross-sectional area of 10^{-3} cm^2 . If $\tau_p = 1 \mu\text{s}$ and $D_p = 10 \text{ cm}^2/\text{s}$, calculate the current with a forward bias of 0.5 V at 300 K .

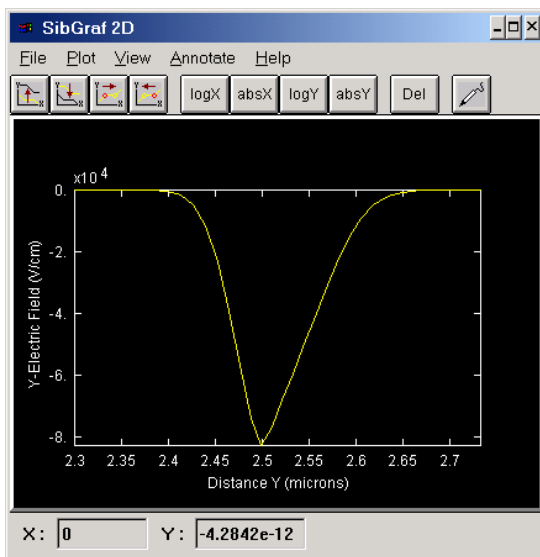


Figure 5.12.1 Electric field under 0 V bias. Graph was zoomed to better show the transition region.

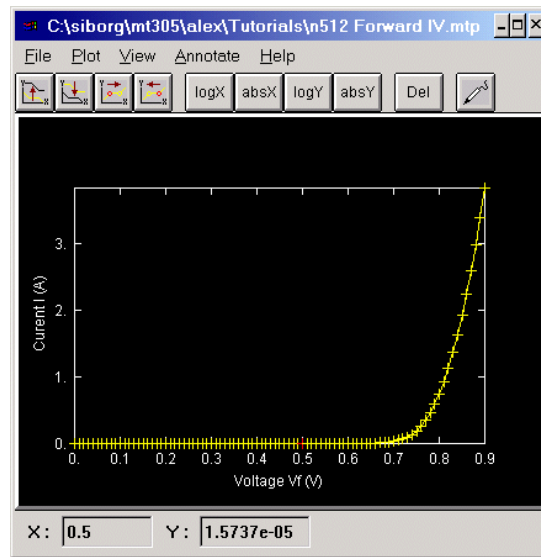


Figure 5.12.2 IV characteristic plot.

Project

The X, Y and Z domains were respectively set to 100, 5 and 1000 μm . The p-side extends in the Y direction from 0 to 2.5 and the n-side from 2.5 to 5 μm with an abrupt junction. $N_d=5 \times 10^{16} \text{ cm}^{-3}$ $N_a=1 \times 10^{17} \text{ cm}^{-3}$. 5 nodes in the X, and 60 nodes in the Y direction were used. No high doping, nor impact ionization effects were included. The constant mobility model was used, with $\mu_n=1000 \text{ cm}^2/\text{V}\cdot\text{s}$ and $\mu_p=384 \text{ cm}^2/\text{V}\cdot\text{s}$ (calculated from diffusion coefficient using Einstein relation). Lifetime of both electrons and holes was set to 1 μs . Default bandgap was used. Two electrodes were specified, one at the top and one at the bottom of the domain. Ten IV points were calculated, starting at 0 V and ending with 1 V forward bias.

Solution

The acceptor doping was chosen to be $N_a=10^{17} \text{ cm}^{-3}$ in order to reduce the spillover effect. Under 0 V bias, figure 5.12.1 shows the electric field. Although spillover is not present, we still see mobile carrier effects at the edges of the transition region. The junction also appears rather symmetric, which is expected as the doping concentrations are comparable.

At 0.5 V forward bias, the status bar of figure 5.12.2 shows that the current is $\sim 1.57 \times 10^{-5} \text{ A}$.

3.7 Problem 5.13

a) Explain physically why the charge storage capacitance is unimportant for reverse-bias junctions. b) Assuming that a GaAs junction is doped to equal concentrations on the n and p sides, would you expect electron or hole injection to dominate in forward bias?

Projects a-b

The projects 5.13a-b have similar geometry and models, and differ by the applied bias. The X, Y and Z domains were respectively set to 100, 2000 and 100 μm . The p-side extends in the Y direction from 0 to 2.5 and the n-side from 2.5 to 5 μm with an abrupt junction. $N_a=N_d=10^{16} \text{ cm}^{-3}$. 5 nodes in the X, and 1000 nodes in the Y direction were used. No high doping, nor impact ionization effects were included. In order to create a GaAs junction, the material properties had to be changed see step 5. on page 37. The bandgap width (E_g), semiconductor dielectric permittivity (ϵ_r), and the electron and hole mobilities (using the constant mobility model), were all set according to GaAs specifications in the book. Lifetime of both electrons and holes was set to 1 μs . The default model for lifetime was used. Two electrodes were specified, one at the top and one at the bottom of the domain. One IV point was calculated at 0 V bias.

Solution

From the electric field diagram in figure 5.13.1, we can see that $x_{n0}=x_{p0}$. This is expected as both sides of the junction are doped equally.

Note that in figures 5.13.1 and 5.13.2, only a narrow space charge region has been plotted.

In figures 5.13.2 and 5.13.3, the concentrations have been plotted at 0 V and 0.5 V forward bias, and different zoom levels.

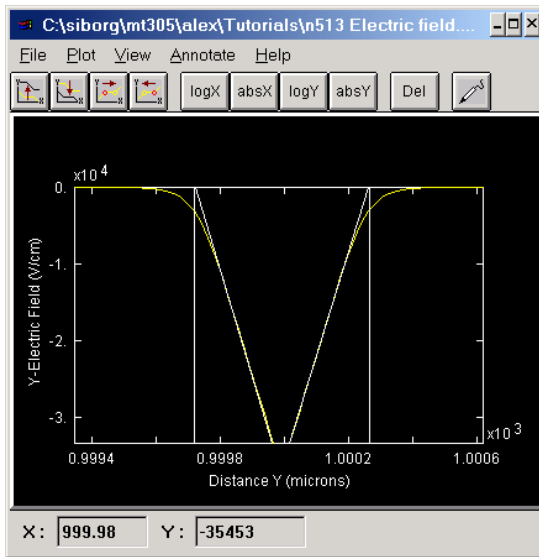


Figure 5.13.1 Close-up of the electric field. Annotation lines mark x_{n0} and x_{p0} . Project a. Graph was zoomed.

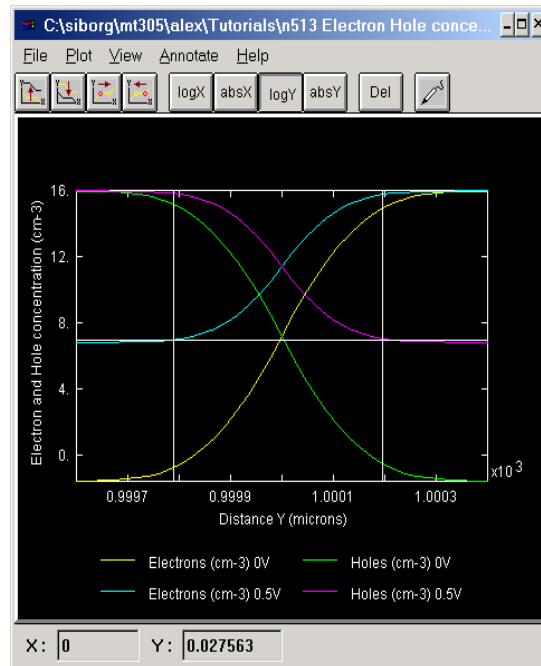


Figure 5.13.2 Logarithm of excess carrier concentrations throughout transition region at 0 V and 0.5 V forward bias. Annotation lines mark x_{p0} and x_{n0} . Green and yellow project a, magenta and cyan project b. Graph was zoomed.

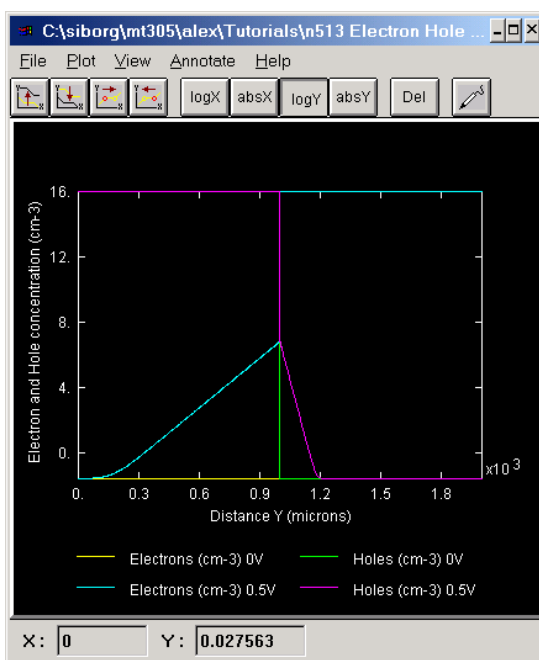


Figure 5.13.3 Logarithm of electron and hole concentrations in a symmetrically doped GaAs junction under 0 V and 0.5 V forward bias. Yellow and green project a, magenta and cyan project b.

Examining injected electron and hole concentrations in figure 5.13.2 at x_{p0} and x_{n0} respectively, we see that they are equal ($\Delta n_p = \Delta p_n$). This is because diffusion across the transition region is governed by carrier concentrations on either side of the junction and by the electrostatic potential barrier. Since the doping concentrations are equal, holes and electrons that are injected across the junction equally at any given bias, provided it is not high-level injection. Although $\Delta n_p = \Delta p_n$, figure 5.13.3 demonstrates that $\delta n(x_p) \neq \delta p(x_n)$. In the large 1000 μm domain we can see the exponential distribution of excess electrons on the p-side, and the much shorter distribution of holes on the n-side. Clearly, the diffusion current due to injected electrons dominates under forward bias.

3.8 Problem 5.14

a) A Si p^+-n junction 10^{-2} cm^2 in area has $N_d=10^{15} \text{ cm}^{-3}$ doping on the n side. Calculate the junction capacitance with a reverse bias of 10 V. b) An abrupt p^+-n junction is formed in Si with a donor doping of $N_d=10^{15} \text{ cm}^{-3}$. What is the depletion region thickness W just prior to avalanche breakdown?

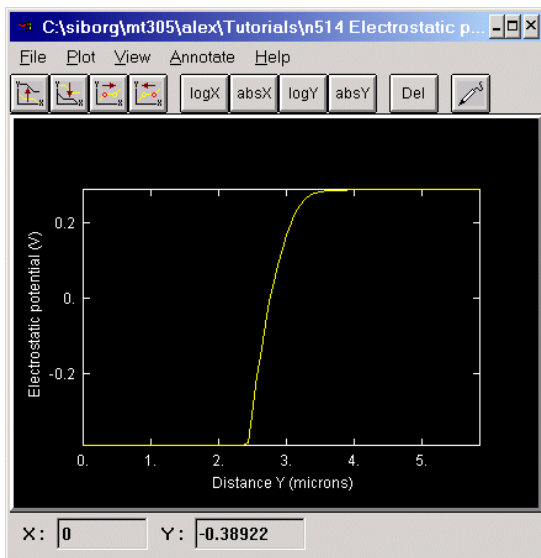


Figure 5.14.1 Electrostatic potential used to find V_0 .
Project a.

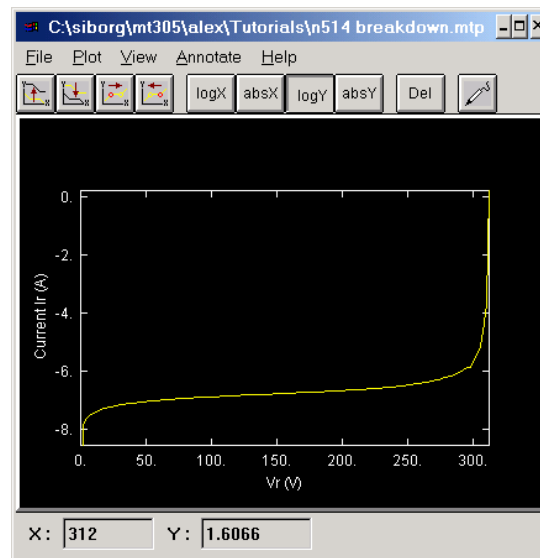


Figure 5.14.2 Reverse IV with breakdown.
Project b.

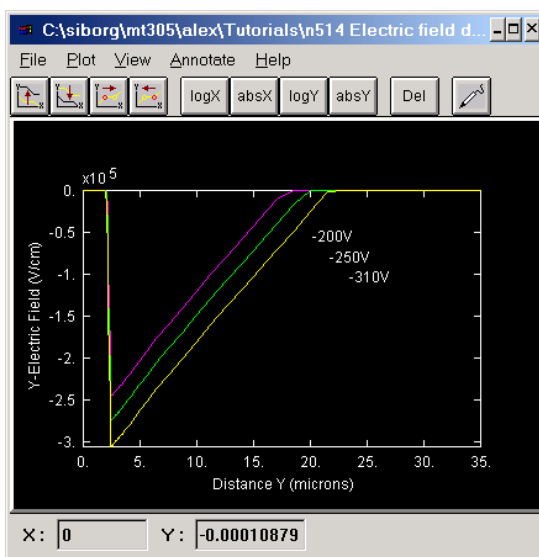


Figure 5.14.3 Electric field at different biases. At -310 V reverse bias, the yellow curve, the depletion region is ~ 19.6 microns. Magenta project c, green project d, yellow project e.

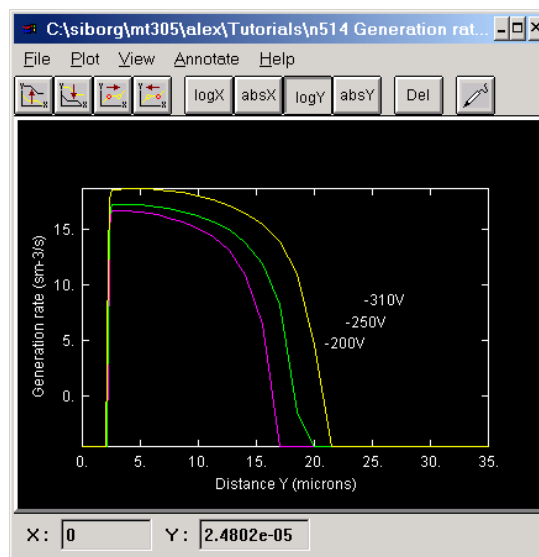


Figure 5.14.4 EHP generation rates at different reverse biases. Magenta project c, green project d, yellow project e.

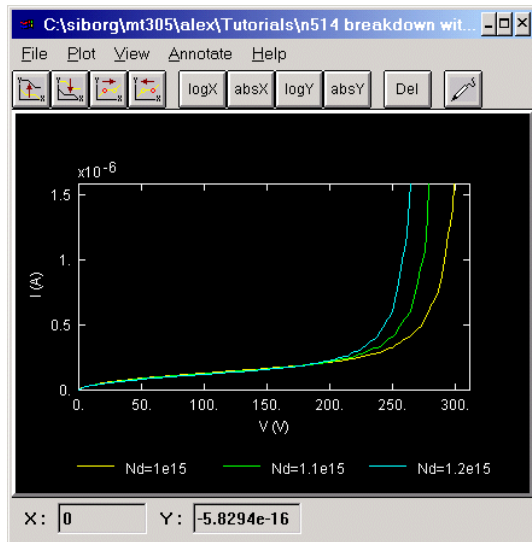


Figure 5.14.5 Avalanche breakdown for different N_d . Zoomed. Yellow project a, green project f, cyan project g.
pF.

Since the junction is lightly doped, it is more likely that avalanche breakdown will occur instead of Zener breakdown. Reverse biasing the junction, we find that avalanche breakdown occurs at ~ -312 V (figure 5.14.2). Biasing the junction with -310 V, the depletion region thickness W just prior to avalanche breakdown is observed to be ~ 19.6 μm (figure 5.14.3, yellow curve). Figure 5.14.3 and 5.14.4 show the effects of increasing reverse bias. As reverse bias increases, W and peak electric field E_0 increase as well. W expands into the lighter doped side. The generation of EHP increases exponentially as we near the breakdown voltage because of carrier multiplication, and therefore is plotted on a log scale.

Figure 5.14.5 shows the effect of changing the doping of the lighter side on avalanche breakdown. As N_d is increased, the peak electric field within W increases, see “Problem 5.10” on page 13 and “Problem 5.15” on page 18. A stronger electric field increases the propability of ionizing collisions inside the transition region. As a result, V_{br} is decreased.

3.9 Problem 5.15

Using equations (5.17) and (5-23), show that the peak electric field in the transition region is controlled by the doping on the more lightly doped side of the junction.

Projects a-e

The projects 5.15a-e all have similar geometry and models, and differ by doping levels. The p-side extends in the Y direction from 0 to 1 and the n-side from 1 to 3 μm with an abrupt junction. The number of nodes used in the X and Y direction were 5 and 60 respectively. No high doping, nor impact ionization effects were included. Default models for mobility, lifetime and bandgap

Projects a-e

The projects 5.14a-e have similar geometry and models, and differ only by the applied bias. The X, Y and Z domains were respectively set to 1000, 35 and 1000 μm . The p-side extends in the Y direction from 0 to 2.5 and the n-side from 2.5 to 35 μm with an abrupt junction. $N_d=10^{15}$ cm^{-3} , $N_a=5 \times 10^{16}$ cm^{-3} . 5 nodes in the X, and 60 nodes in the Y direction were used. No high doping effects were included. In order to observe avalanche breakdown, the impact ionization model was included. Two electrodes were placed, one at the top and one at the bottom of the domain. The junction was then reverse biased at various voltages.

Solution

From figure 5.14.1, V_0 was calculated to be ~ 0.68 V. Having V_0 , we calculate C_j using the formula given in the book. For our p^+-n junction C_j is found to be ~ 28

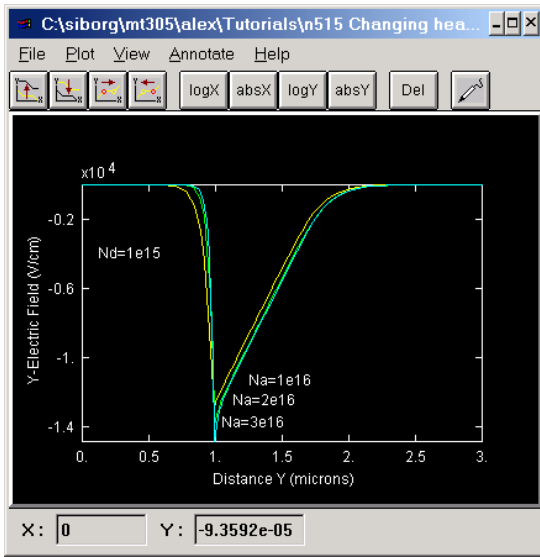


Figure 5.15.1 Changes in peak electric field E_0 due to variations in N_a .
Yellow project a, green project b, cyan project c.

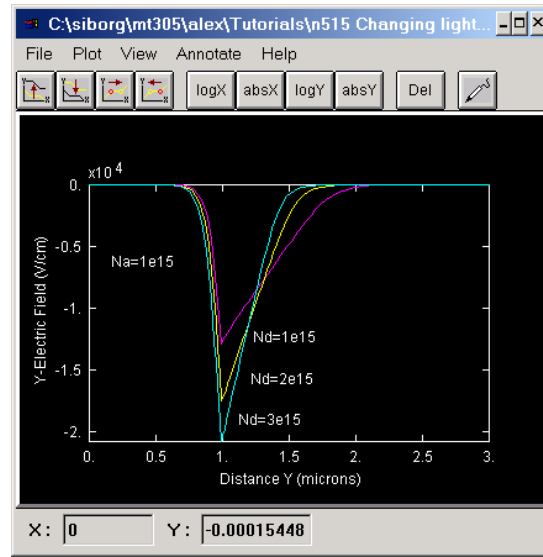


Figure 5.15.2 Changes in peak electric field E_0 due to variations in N_d .
Magenta project a, yellow project d, cyan project e.

were used. Two electrodes were specified at the top and bottom of the domain. Only one IV point was calculated at 0 V bias.

Solution

In an p^+n junction, the depletion region extends further into the n -type, lighter doped side (to the right, in the figures). Thus the lighter doped side contributes more to the peak electric field. Figure 5.15.1 demonstrates the effect of varying the doping on the heavier doped side. Ignoring spillover, one can see that variations in N_a have very little effect on E_0 . This may be seen from Eq.(5-17) and Eq.(5-23); varying N_a (the heavier doped side) does little to change the location of x_{p0} and x_{n0} , hence E_0 remains the same. If, as in figure 5.15 2, the doping on the lighter doped side is changed, the effect on E_0 becomes pronounced; as Eq.(5-23) predicts, the change in x_{p0} is small but x_{n0} changes considerably. As a result, extrapolated E_0 changes as well.

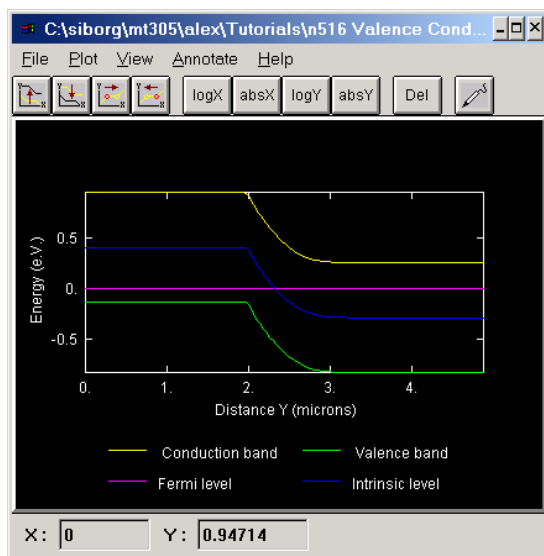


Figure 5.16.1 Equilibrium band diagram.

3.10 Problem 5.16

An abrupt Si p-n junction has the following properties at 300K: $A=10^{-4}cm^2$

<u>p-side</u>	<u>n-side</u>
$N_a=10^{17} cm^{-3}$	$N_d=10^{15}$
$\tau_n=0.1 \mu s$	$\tau_p=10$
$\mu_p=200 cm^2/V-s$	$\mu_n=1300$
$\mu_n=700$	$\mu_p=450$

Problems

Draw the equilibrium band diagram for this junction, including numerical values for the Fermi level position relative to the intrinsic level on each side. Find the contact potential from the diagram and check your answer with the analytical expression for V_0 .

Project

The X, Y and Z domains were respectively set to 10000, 10 and 10000 μm . The p-side extends in the Y direction from 0 to 2 and the n-side from 2 to 10 μm with an abrupt junction. $N_a=10^{17} \text{ cm}^{-3}$, $N_d=10^{15} \text{ cm}^{-3}$. 5 nodes in the X, and 60 nodes in the Y direction were used. No high doping, nor impact ionization effects were included. In order to achieve the specified mobilities, the bipolar mobility model was used, see step 9. on page 37. Lifetimes of both electrons and holes were set to the specified values. Default bandgap was used. Two electrodes were placed, one at the top and one at the bottom of the domain. One IV point at 0V bias was calculated.

Solution

Contact potential may be calculated from the height of the conduction band step in figure 5.16.1; $\sim 0.947\text{V} - (\sim 0.251\text{V}) = \sim 0.696 \text{ V}$. Analytically, $V_0=0.695 \text{ V}$. Since the junction is at equilibrium, the electron and hole quasi-Fermi levels coincide and are equal to 0 eV. Relative to the intrinsic level, on the p side, the Fermi level is at -0.407 eV. On the n side, the Fermi level is at 0.288 eV relative to the intrinsic level.

3.11 Problem 5.19

A Si p-n junction with cross sectional area, $A=0.001 \text{ cm}^2$ is formed with $N_a=10^{15} \text{ cm}^{-3}$, $N_d=10^{17} \text{ cm}^{-3}$. Calculate a) Contact potential, V_0 . b) Space charge width at equilibrium (zero bias). c) Current with a forward bias of 0.5 V. Assume that the current is diffusion dominated. Assume $\mu_n=1500 \text{ cm}^2/\text{V-s}$, $\mu_p=450 \text{ cm}^2/\text{V-s}$, $\tau_n=\tau_p=2.5 \mu\text{s}$. Which carries most of the current, electrons or holes and why? If you wanted to double the electron current, what should you do?

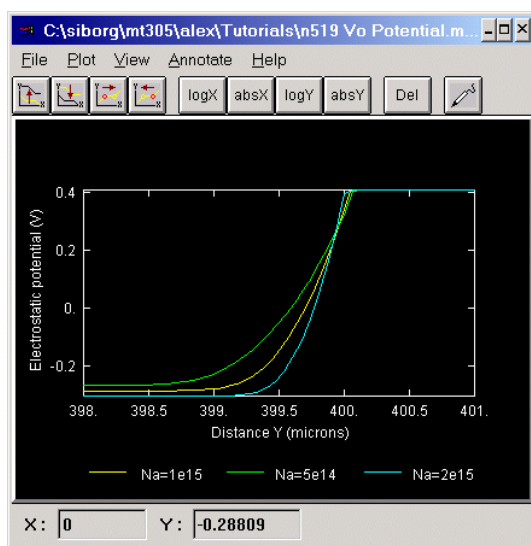


Figure 5.19.1 Electrostatic potential under 0 V bias for the long diode.

$V_0 \cong 0.695 \text{ V}$ from yellow curve. Yellow project a, cyan project b, green project c. Zoomed.

or holes and why? If you wanted to double the electron current, what should you do?

Projects a-i

The projects 5.19a-i have similar geometry and models, and differ only by the applied bias and N_a doping. The X, Y and Z domains were respectively set to 100, 600 and 1000 μm , which made this diode a long diode.. The p-side extends in the Y direction from 0 to 400 and the n-side from 400 to 600 μm with an abrupt junction. The donor doping was kept at $N_d=10^{17} \text{ cm}^{-3}$. 4 nodes in the X, and 300 nodes in the Y direction were used. No high doping, nor impact ionization effects were included. The constant mobility model was used, with $\mu_n=1500 \text{ cm}^2/\text{V-s}$ and $\mu_p=450 \text{ cm}^2/\text{V-s}$. Lifetime of both electrons and holes was set to 2.5 μs . Default bandgap was used. Two electrodes were specified, one

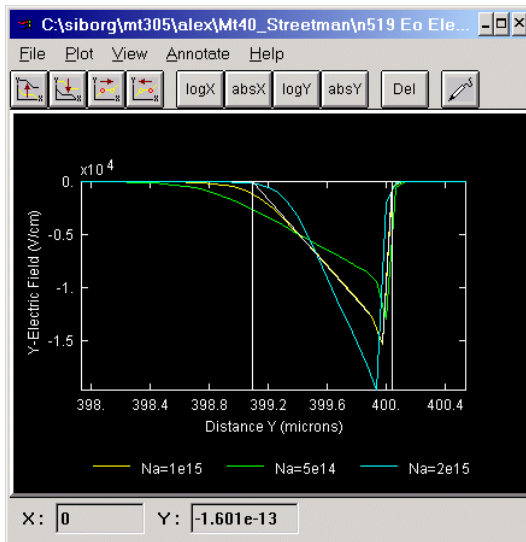


Figure 5.19.2 Under 0 V bias, depletion region width $\sim 0.95 \mu\text{m}$ for yellow curve. Long diode. Yellow project a, cyan project b, green project c. Zoomed.

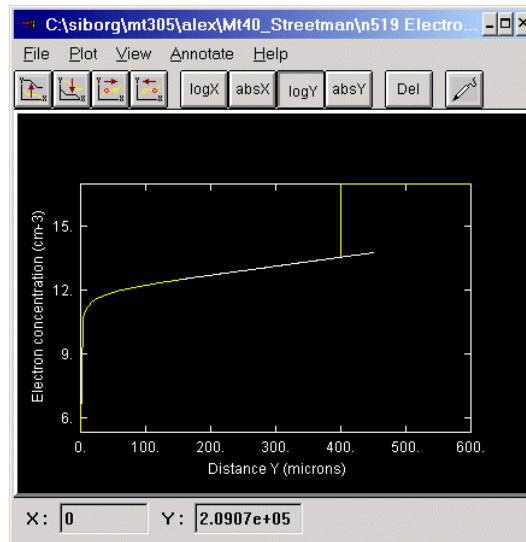


Figure 5.19.3 Logarithm of electron concentration on the p-side under 0.5 V forward bias. Long diode. Project g.

at the top and one at the bottom of the domain. Projects 5.19as-hs deal with the short version of this diode. The short diode differs only in that it's Y domain is $3 \mu\text{m}$ and not $600 \mu\text{m}$ like for the long diode. P side from 0 to 2, n side from 2 to $3 \mu\text{m}$.

Solution for the long Diode

The contact potential $V_0 \cong 0.695 \text{ V}$ is calculated from the 0 V bias equilibrium state electrostatic potential diagram in figure 5.19.1. The figure also shows the effect of changing the lighter side

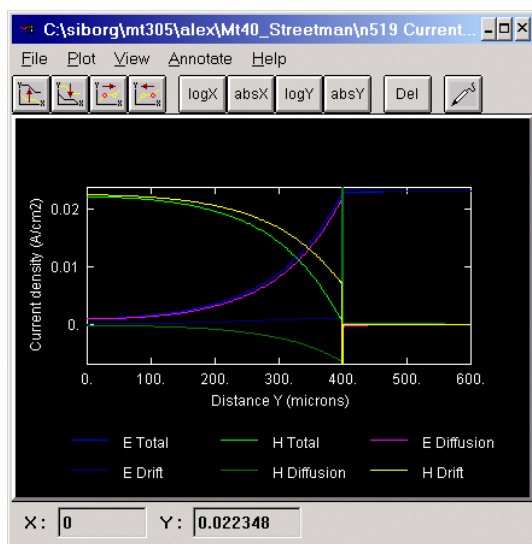


Figure 5.19.4 Current densities for long diode. The hole drift current is yellow. Project g. Zoomed.

doping N_a see “Problem 5.10” on page 13 and “Problem 5.15” on page 18. Increasing N_a from $1 \times 10^{15} \text{ cm}^{-3}$ to $2 \times 10^{15} \text{ cm}^{-3}$ results in a greater V_0 . Decreasing N_a results in a smaller V_0 . The electric field in figure 5.19.2 may be used to calculate the depletion region width of $\sim 0.95 \mu\text{m}$. Increasing N_a results in a smaller depletion region, while a decrease in N_a results in a wider depletion region; as N_a decreases, the junction extends deeper into the lighter doped side as more positive charge must be uncovered to balance the negative charge and for the device to be in equilibrium.

It is known that the junction is $p\text{-n}^+$, therefore electrons carry most of the current near the junction, it is also known that current is diffusion dominated. In order to calculate the current at the junction Eq (5-34) may be

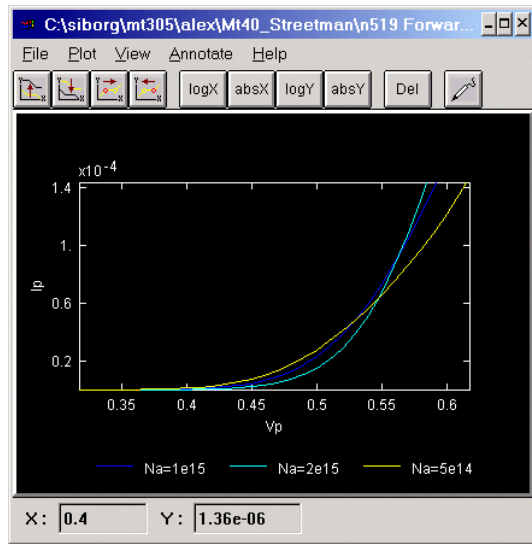


Figure 5.19.5 IV characteristic for long diode. Yellow project d, cyan project e, green project f. Zoomed.

used, but we still need L_n and Δn_p . The location of the depletion region edge may be obtained either from the electric field diagram, or the logarithm of the electron concentration as in figure 5.19.3; on a logarithmic scale, exponential functions are linear. The concentration of excess electrons on the p side decays exponentially away from the junction, and so the junction ends where the exponential begins. An annotation line in figure 5.19.3 clearly shows that the electron concentration behaves exponentially on the p side. Zooming into the junction area, it is found that the edge of the depletion region is at $\sim 398.91 \mu\text{m}$, with $\Delta n_p \sim 3.5 \times 10^{13} \text{ cm}^{-3}$. A similar depletion region edge may be obtained from the electric field diagram.

Recalling eq(5-31), L_n may be calculated from any straight portion (exponential) of the logarithmic graph in figure 5.19.3. Using the probe tool, L_n is found to be $100.5 \mu\text{m}$. L_n may also be calculated from it's definition to be $\sim 99 \mu\text{m}$. Now, using Eq (5-34), we can calculate electron current to be $2.21 \times 10^{-2} \text{ A}$. Figure 5.19.4 shows the components of current throughout the device. Notice that near the junction electron diffusion dominates current, but far from the junction it is hole drift which dominates. By zooming and using the probe tool, the electron current density at the junc-

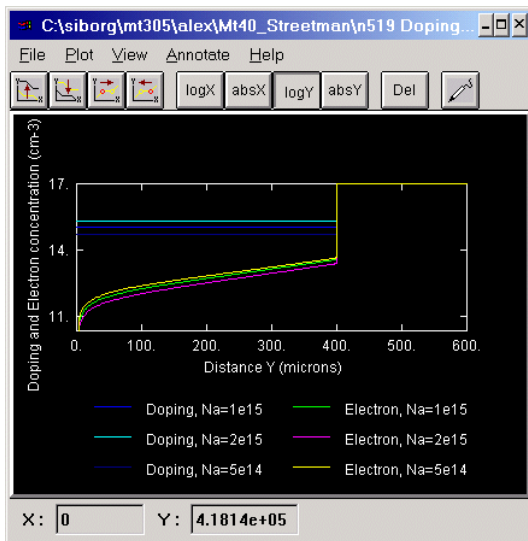


Figure 5.19.6 Logarithm of electron and doping concentrations on the p side under 0.5 V forward bias for the long diode. Dark blue and yellow project g, cyan and magenta project h, blue and green project i. Zoomed.

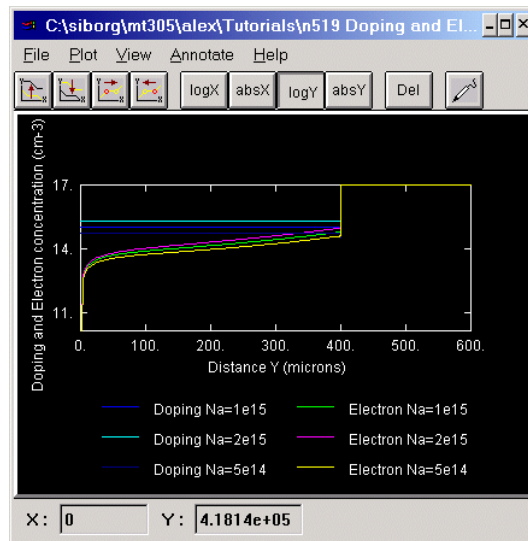


Figure 5.19.7 Logarithm of electron and doping concentrations on the p side under 0.7 V forward bias for the long diode. Green and dark blue project d, magenta and cyan project e, dark green and yellow project f. Zoomed.

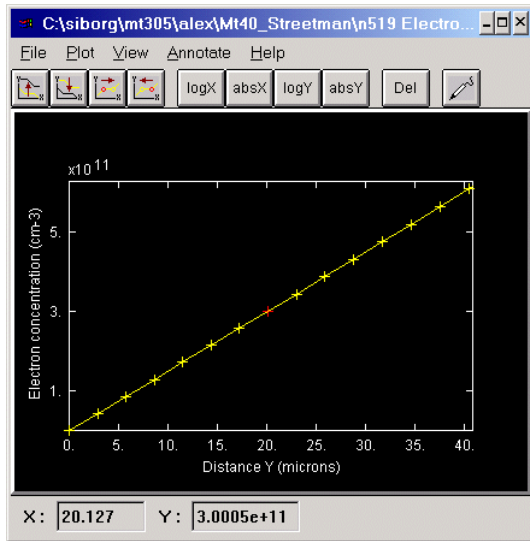


Figure 5.19.8 Electron concentration under 0.5 V forward bias for the long diode.

Project g. Calculation of slope gives $1.5 \times 10^{10} \text{ cm}^{-3}/\mu\text{m}$ and $n(x) = 3.0 \times 10^{11}$. Zoomed.

which decrease the current. At lower voltages, resistance plays a lesser role. At 0.4 V, for $N_a = 10^{15} \text{ cm}^{-3}$, $I \sim 0.709 \times 10^{-3} \text{ mA}$, for $N_a = 5 \times 10^{14} \text{ cm}^{-3}$ $I \sim 1.36 \times 10^{-3} \text{ mA}$. At higher voltages resistance plays a bigger role and figure 5.19.5 shows that the effects of resistance dominate beyond $\sim 0.54 \text{ V}$ where the decrease in current due to resistance is greater than the increase in current due to lighter doping.

Unlike in the short diode, the resistance in the long diode reduces the effective potential across the

tion is found to be $2.23 \times 10^{-2} \text{ A/cm}^2$.

In order to double electron current it is necessary to decrease N_a by $1/2$; the new N_a will be $5 \times 10^{14} \text{ cm}^{-3}$. Although this might at first seem counter intuitive, an analysis of the formulas that are involved clears any doubt. According to Eq(5.8), a decrease in N_a causes a decrease in V_0 (figure 5.19.1). Eq(5.26) states that a decrease in V_0 will result in an increased n_p . By Eq(5.30), a larger n_p will cause Δn_p to increase. An increase in Δn_p will result in a larger electron diffusion current. Figure 5.19.5 shows the forward IV characteristic of the junction and the effect on current of either an increase or a decrease in N_a . It should be noted that because we are dealing with a long diode, the effects of resistance become visible. Changes in doping are countered by the effects of resistance; a decrease in N_a increases the current but also increases the resistance

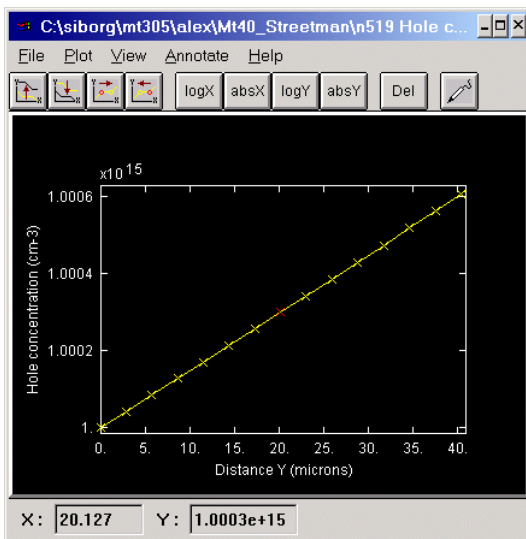


Figure 5.19.9 Hole concentration under 0.5 V forward bias for the long diode.

Project g. Calculation of slope gives $1.48 \times 10^{10} \text{ cm}^{-3}/\mu\text{m}$ and $p(x) = 1.0 \times 10^{15}$. Zoomed.

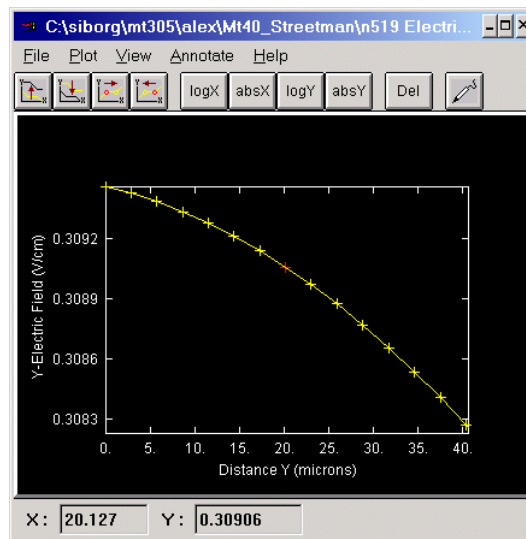


Figure 5.19.10 Electric field under 0.5 V forward bias for the long diode.

Project g. Zoomed.

Problems

junction. As a result, the excess carrier concentrations for the short and long diodes are different at similar voltages. Figures 5.19.6 and 5.19.7 show Δn_p at 0.5 and 0.7 V. At 0.7 V the electron concentration in the long diode is less than in the short diode at the same voltage. High-level injection does not occur to the same extent in the long diode as it does in the short diode at 0.7 V. The reason is that because of resistance, the effective potential across the junction is reduced. As a result, greater voltages are needed for high-level injection to occur.

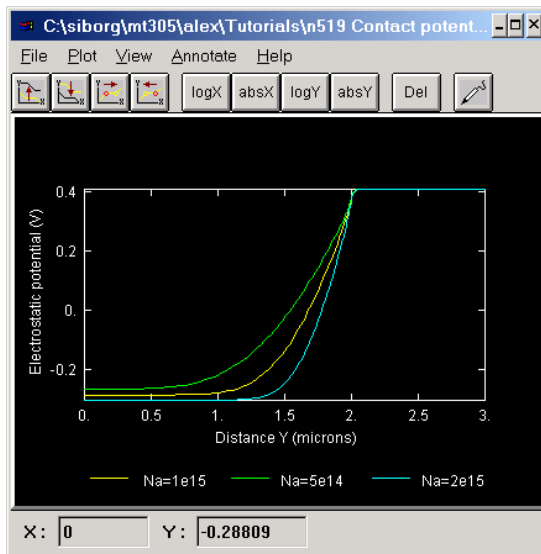


Figure 5.19.11 Electrostatic potential under 0 V bias for the short diode.

$V_0 \approx 0.695$ V from yellow curve. Yellow project as, cyan project bs, green project cs.

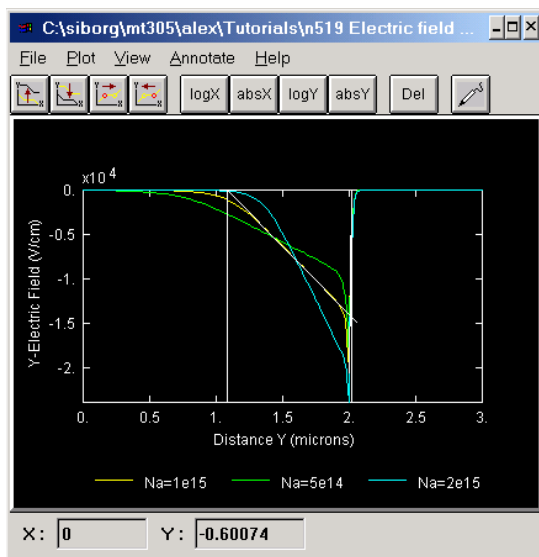


Figure 5.19.12 Electric field for short diode. W is the same for short and long diode. Yellow project as, cyan project bs, green project cs.

To calculate the current deep in the p-side, we could use Eq (4-23). Several constants and variables are needed to calculate both the drift and diffusion components of $J_n(x)$ and $J_p(x)$. The constants μ_n , μ_p , and thus D_n , D_p (through Einstein relation) are given in the problem. It remains to find $n(x)$, $p(x)$, $E(x)$, $dn(x)/dx$ and $dp(x)/dx$. All these values are easily obtained. Figure 5.19.8 shows the electron concentration on the p side under a 0.5V forward bias. From this figure, $n(x)$ and $dn(x)/dx$ may be calculated. To find $dn(x)/dx$, simply find a straight portion of the graph and calculate rise/run (be careful with the units). In our example, $dn(x)/dx = 1.5 \times 10^{10} \text{ cm}^{-3}/\mu\text{m}$ and $n(x) = 3.0 \times 10^{11}$. Repeat for hole concentration to obtain $dp(x)/dx = 1.48 \times 10^{10} \text{ cm}^{-3}/\mu\text{m}$ and $p(x) = 1.0 \times 10^{15}$ (figure 5.19.9). Figure 5.19.10 shows the electric field. $E(x)$ is 0.309 V/cm. Make sure that $n(x)$, $p(x)$, $E(x)$, $dn(x)/dx$ and $dp(x)/dx$ are all taken at the same location inside the device. For this example, all the measurements were taken $\sim 20 \mu\text{m}$ from the surface.

Having worked out the components of J_n , it is found that $J_n = 9.57 \times 10^{-4} \text{ A/cm}^2$ is less than $J_p = 2.20 \times 10^{-2} \text{ A/cm}^2$. It was also found that hole drift current $2.23 \times 10^{-2} \text{ A/cm}^2$ is greater than hole diffusion current $2.77 \times 10^{-4} \text{ A/cm}^2$. Therefore, in this device electron diffusion current is not zero deep in the p side, however it is small compared to hole drift current. This is because the device was not made long enough. All these findings are shown in figure 5.19.4.

Solution for the Short diode

The contact potential V_0 and depletion region width discussion is the same for the short diode as it is for the long diode. This is apparent if one recalls the ana-

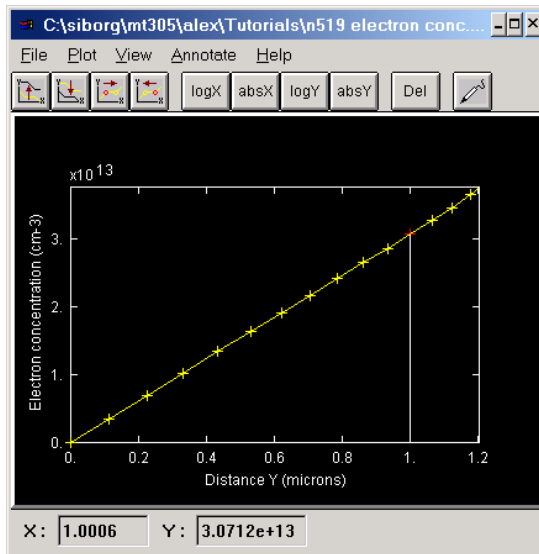


Figure 5.19.13 Electron concentration under 0.5 V forward bias.
Zoomed. Project gs. Calculation of slope gives $3.05 \times 10^{17} \text{ cm}^{-3}/\mu\text{m}$. $n(x) = 3.07 \times 10^{13}$.

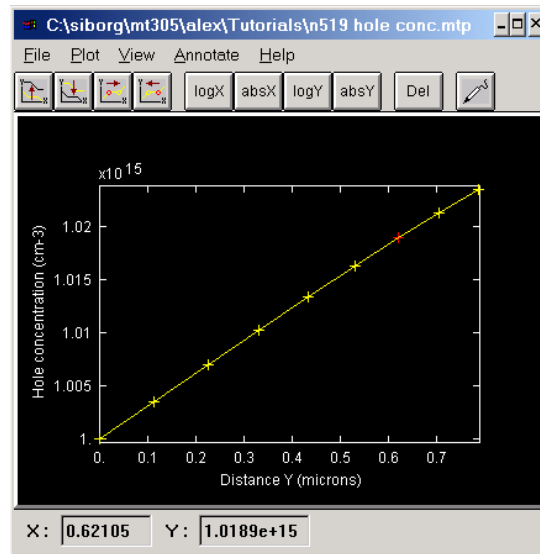


Figure 5.19.14 Hole concentration under 0.5 V forward bias
Zoomed. Project gs. Calculation of slope gives $3.42 \times 10^{17} \text{ cm}^{-3}/\mu\text{m}$. $p(x) = 1.02 \times 10^{15}$.

lytical expressions for V_0 and W . Figures 5.19.11 and 5.19.12 show the equilibrium electrostatic potential and electric field.

Because this diode is short, we cannot use eq(5-34) to calculate current. Eq(5-34) assumes a long diode with exponential excess carrier decay. We must use the more general Eq(4-23) to find the drift and diffusion components of current. Several constants and variables are needed to calculate

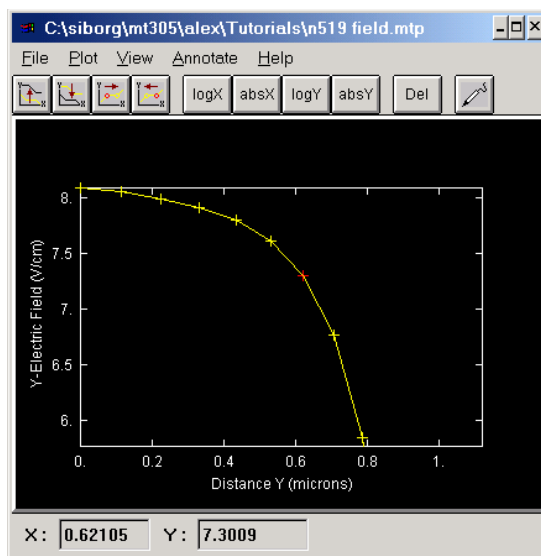


Figure 5.19.15 Electric field under 0.5 V forward bias.
Zoomed. Project gs.

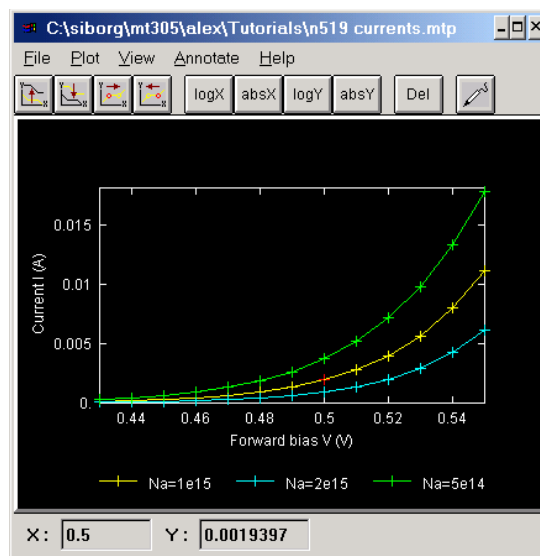


Figure 5.19.16 IV characteristic for short diode.
Yellow project ds, cyan project es, green project fs.

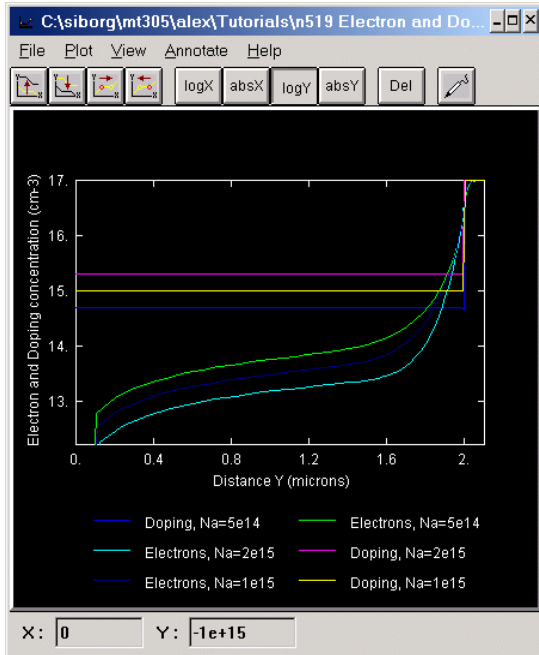


Figure 5.19.17 Logarithm of electron and doping concentrations on the p side under 0.5 V forward bias for the short diode. Dark blue and yellow project gs, cyan and magenta project hs, blue and green project is.

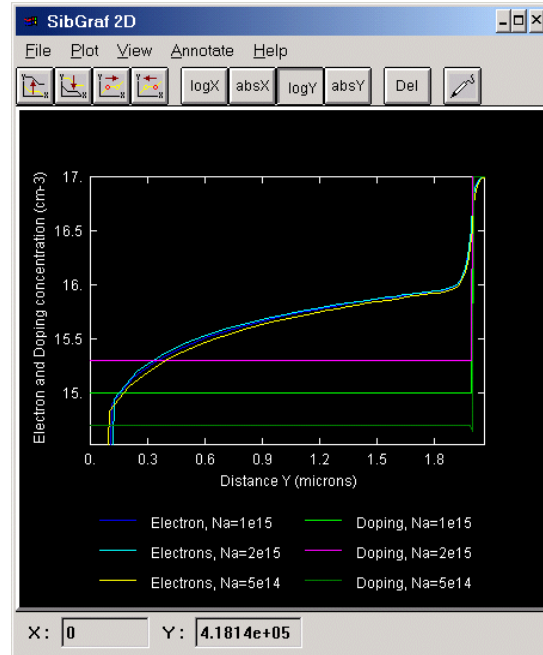


Figure 5.19.18 Logarithm of electron and doping concentrations on the p side under 0.7 V forward bias for the short diode. Green and dark blue project ds, magenta and cyan project es, dark green and yellow project fs.

both the drift and diffusion components of $J_n(x)$ and $J_p(x)$. The constants μ_n , μ_p , and thus D_n , D_p (through Einstein relation) are given in the problem. It remains to find $n(x)$, $p(x)$, $E(x)$, $dn(x)/dx$ and $dp(x)/dx$. All these values are easily obtained. Figure 5.19.13 shows the electron concentra-

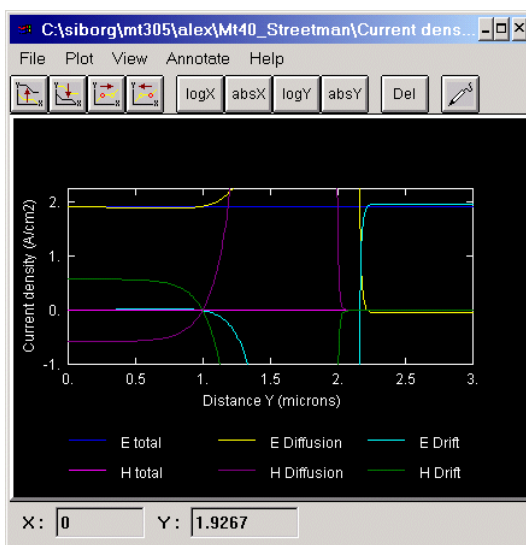


Figure 5.19.19 Current densities for short diode. The electron diffusion current density is yellow. Project gs. Zoomed.

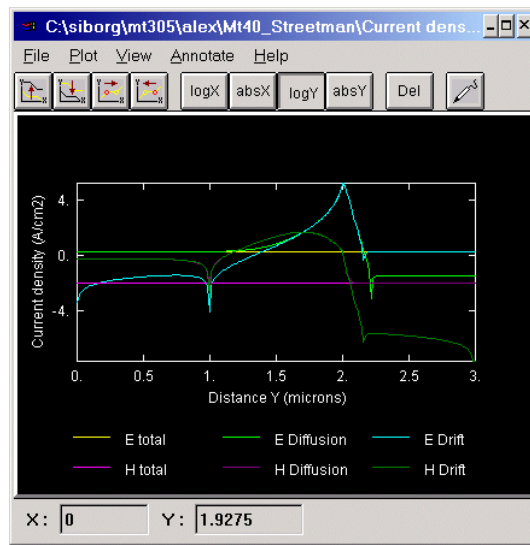


Figure 5.19.20 Logarithm of current densities for short diode. Logarithmic scale. Project gs. Zoomed.

tion on the p side under a 0.5 V forward bias. From this figure, $n(x)$ and $dn(x)/dx$ may be calculated. To find $dn(x)/dx$, simply find a straight portion of the graph and calculate rise/run (be careful with the units). In our example, $dn(x)/dx = 3.05 \times 10^{17} \text{ cm}^{-3}/\mu\text{m}$ and $n(x) = 1.911 \times 10^{13}$. Repeat for hole concentration to obtain $dp(x)/dx = 3.42 \times 10^{17} \text{ cm}^{-3}/\mu\text{m}$ and $p(x) = 1.02 \times 10^{15}$ (figure 5.19.14). Figure 5.19.15 shows the electric field diagram. $E(x)$ is 7.3 V/cm. Make sure that $n(x)$, $p(x)$, $E(x)$, $dn(x)/dx$ and $dp(x)/dx$ are all taken at the same location inside the device. In this example, a depth of $\sim 0.62 \mu\text{m}$ was used.

Having worked out the components of J_n , it is found that electron diffusion current 1.9 A/cm^2 is greater than electron drift current $3.35 \times 10^{-2} \text{ A/cm}^2$. It is also found that $J_n = 1.93 \text{ A/cm}^2$ is larger than $J_p = 1.17 \text{ A/cm}^2$. Therefore it must be that current is diffusion dominated and that electrons carry most of the current. Figure 5.19.19 shows the electron and hole drift and diffusion components of current. Electron diffusion is the largest.

The reasons for decreasing N_a by $\frac{1}{2}$ (now $N_a = 5 \times 10^{14} \text{ cm}^{-2}$) are the same as those for the long diode. Figure 5.19.16 shows the effect on current of either an increased or a decreased N_a . Just as predicted, it is a decreased N_a which results in larger current; for $N_a = 10^{15} \text{ cm}^{-2}$ at 0.5 V forward bias $I \cong 1.9 \text{ mA}$, for $N_a = 5 \times 10^{14} \text{ cm}^{-2}$ $I \cong 3.7 \text{ mA}$. The effects of resistance are not noticeable in the short diode as they were previously in the long diode.

The effects of high-level injection may be seen in Figure 5.19.17 and 5.19.18. High-level injection occurs past a certain voltage when the concentration of injected minority carriers becomes comparable to the doping concentration. High-level injection is not taken into account by the formulas used in the book. In this junction, high-level injection is achieved by a forward bias of 0.7 V. At this voltage, high-level injection prevents any significant changes in current due to changes in doping. As the figure 5.19.17 demonstrates, at 0.5 V changes in N_a result in significant

changes of electron concentration which, in turn, changes current. On the other hand, in figure 5.19.18, at 0.7 V, no such effect is observed.

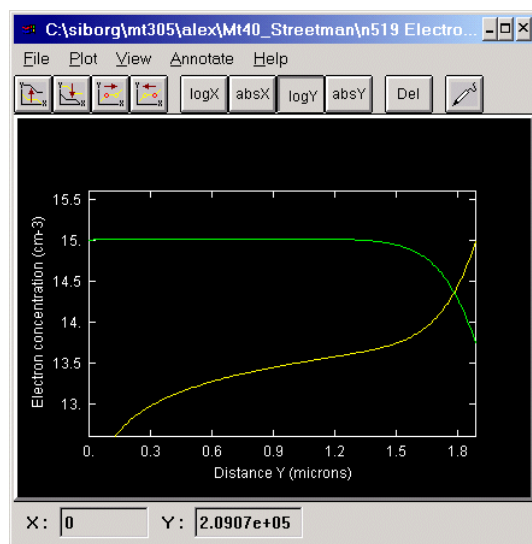


Figure 5.19.21 Logarithm of electron and hole concentrations near transition region. Zoomed. Project gs.

Figure 5.19.19 shows all the current components. The yellow curve shows the dominant electron diffusion component of current. Notice how different the current densities are in the short and long diode. Figure 5.19.20 shows all the currents on a logarithmic scale. Electron current is visibly greater than hole current; this is expected as the junction is $p-n^+$. Also note that near the transition region, the majority carrier current components appear to be almost equal. Drift and diffusion currents go in opposite directions. Under equilibrium conditions, diffusion and drift currents must cancel out. The reason the two components are so sim-

Problems

ilar in this example is because the applied 0.5 V forward bias is small compared with the equilibrium state.

The logarithm of the electron concentration on the p side in figure 5.19.21 shows no straight portions, and hence no exponential decay. This is an indication that the diffusion length of electrons exceeds the length of the p side. In fact if calculated, L_n is $\sim 100 \mu\text{m}$. This also explains the current densities in figure 5.19.19; electron diffusion current doesn't really seem to decrease throughout the p side. As well, electron and hole concentrations near the transition region can be seen to be affected by mobile carrier effects which cause the edges of the transition region not to be sharp. One can also see how electron concentration falls near the electrode.

The equations in the book are built on the assumption that the diode is long, and so the provided diode equation eq(5-34) will give incorrect results if used for short diodes. The current equations for long and short diodes differ very slightly. To calculate electron current, the long diode equation uses the diffusion length L_n , whereas the short diode equation uses the length of the p side that has no electric field. The ratio $I_{n \text{ long}} / I_{n \text{ short}} = L / L_n$, where L is the length of the p side with no field, should hold. By zooming figure 5.19.12, the length of the p side with minimal field can be seen to be $\sim 0.5 \mu\text{m}$. Evaluating eq(5-34) with $L_n = 0.00005 \text{ cm}$, we get that $I_{n \text{ short}} = 4.35 \text{ A}$. Previously, $I_{n \text{ long}}$ was calculated to be $2.12 \times 10^{-2} \text{ A}$. Performing the division we find that $I_{n \text{ long}} / I_{n \text{ short}} = L / L_n = 0.0051$.

3.12 Problem 5.25

A p^+-n Si diode ($V_0 = 0.956 \text{ V}$) has a donor doping of 10^{17} cm^{-3} and an n-region width = $1 \mu\text{m}$. Does it break down by avalanche or punch-through?

Projects a-f

The projects 5.25a-f have similar geometry and models, and differ only by the applied bias and N_d doping as specified on the graphs below. N_a was kept at $2.4 \times 10^{19} \text{ cm}^{-3}$. The X, Y and Z domains were respectively set to 1, 2 and $10000 \mu\text{m}$. The p-side extends in the Y direction from 0 to 1 and the n-side from 1 to $2 \mu\text{m}$ with an abrupt junction. 5 nodes in the X, and 200 nodes in the Y direction were used. No high doping effects were included. In projects where avalanche breakdown occurs, the impact ionization model was included. The electron and hole lifetimes were set to $0.1 \mu\text{s}$ and $10 \mu\text{s}$ respectively. Two electrodes were placed, one at the top and one at the bottom of the domain. The junction then was reverse biased for various donor concentrations.

Solution

Given that $V_0 = 0.956 \text{ V}$ and $N_d = 10^{17} \text{ cm}^{-3}$, N_a was calculated to be $2.4 \times 10^{19} \text{ cm}^{-3}$. Figure 5.25.1 shows reverse IV characteristics, and figure 5.25.2 shows electric fields. As expected, the field extends further into the n region. For all the curves, $N_a = 2.4 \times 10^{19} \text{ cm}^{-3}$.

The green and magenta curves of figure 5.25.1 and the yellow, light green and dark green curves of figure 5.25.2 correspond to $N_d = 10^{17} \text{ cm}^{-3}$. For this concentration, the IV characteristics show that the diode breaks down by avalanche at $V_f \cong 13 \text{ V}$. The electric field at breakdown is shown by

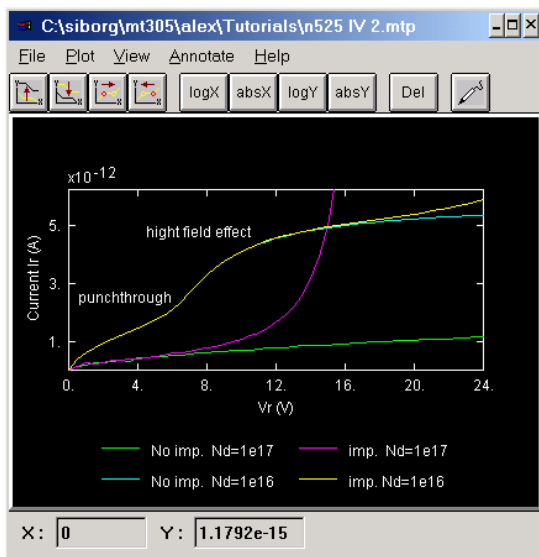


Figure 5.25.1 Reverse IV characteristic. For different donor concentrations with and without impact ionization. Green project a, magenta project b, cyan project c, yellow project d.

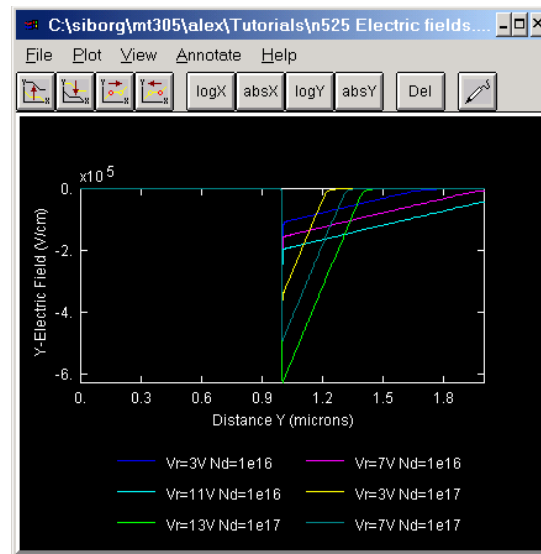


Figure 5.25.2 Transition region width is clearly visible in electric field diagrams. Blue magenta cyan projects e, yellow green dark green projects f.

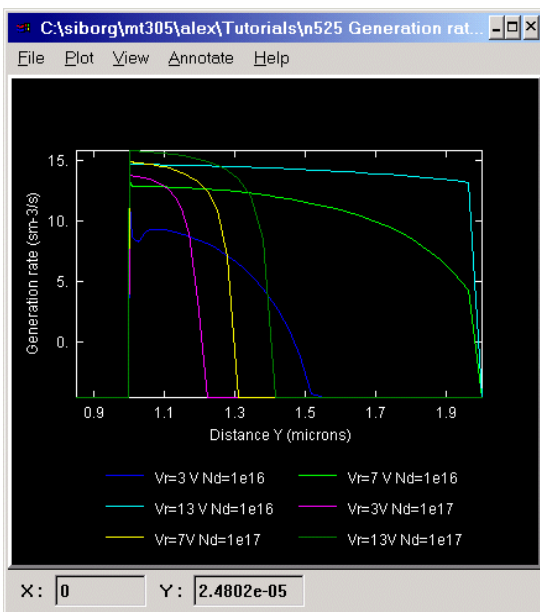


Figure 5.25.3 Logarithmic plot of the EHP generation rate. Light blue green cyan projects e, magenta yellow dark blue projects f.

the light green electric field curve. Clearly punch-through has not occurred.

If N_d is decreased to 10^{16} cm^{-3} , the yellow and cyan curves of figure 5.25.1 and the blue, cyan and magenta curves of figure 5.25.2 are obtained. For this concentration, the IV characteristics show that the diode breaks down by punch-through at $V_r \cong 7 \text{ V}$. The electric field at breakdown is shown by the magenta electric field curve. Note that at punch-through breakdown the transition region on the lighter doped side has extended throughout the whole n region; the cause of the breakdown. Beyond V_{br} , the device ceases to function as a p-n junction and starts to behave like a capacitor. Further increase in V_r results in a linear increase in current. Linearity persists until electron drift velocity starts to saturate, at which point the current starts to level off. If impact ionization is included in the model, avalanche breakdown is visible (tail of the

Problems

With the impact ionization model included, Figure 5.25.3 shows the EHP generation rates. Notice how the generation occurs right inside the transition region; that is where the electrons are being accelerated by the electric field. The evenly spaced curves suggest an exponential increase in the generation rate. See “Problem 5.14” on page 16 for more about avalanche breakdown.

4. Small MicroTec Tutorial

This tutorial is designed to give a first time user a general feel for the program. Please refer to the [Manual](#) with further questions.

MicroTec™ is a two dimensional semiconductor process and device simulator for silicon devices that runs under Windows™. A finite difference analysis is performed through the structure and the results are presented in a flexible and easy to understand graphical format. MicroTec is fast and easy to use, with a short learning curve.

4.1 Tech Stuff

MicroTec stores all project related files in the same directory as the MicroTec executable. The project files have extensions ***.dbf** ***.mdx**. These files may be backed up and restored.

4.2 Using MicroTec

MicroTec has three different modes of operation, which will be presented in the order they are generally encountered.

4.2.1 Project selection/creation screen

This is the initial screen that the user sees once MicroTec has been started.

- A new project may be created by either adding a project, or copying an existing project.
- To create a new project, type in a project name, choose a method that suits the requirements of the project, give the project a brief description (optional), and click **Add**.
- To copy an existing project, select an existing project that suits the requirements, and click **Copy**. A new project with “(copy)” appended to the name will be created.
- One of four methods is chosen for the project:

1. SiDif

Simulation of Diffusion is used to simulate fabrication processes.

2. SemSim

Semiconductor Simulator is used to simulate semiconductor devices.

3. MergIC

Merge IC is a program that merges fragments of IC elements. It links SiDif and SemSim. SiDif>MergIC>SemSim; accomplished by specifying input files in MergIC (input is output from SiDif) and in SemSim (input is output from MergIC). For MergIC and SemSim, these inputs may be specified in “Project Settings” inside specific directives.

4. Batch Mode

While either SiDif or SemSim may be run strictly on their own, it is also possible to fabricate a semiconductor device (SiDif) from several fragments (MergIC) and put it through it’s paces (SemSim); batch mode allows the stringing of these methods one after the other.

- It is helpful to give each project a brief description.
- Once a project has been created, **Update** must be pushed following any changes made to either the project name or description.
- It is always possible to return to project selection by clicking **Select Project** tab.

4.2.2 Project settings and execution.

Once a project has been selected or created, clicking on the Project Settings tab will take the user to the next stage. This is the factory and laboratory, where values are set and devices are created and tested.

The project settings screen is comprised of a directives and subdirectives tree with parameters leaves.

1. Directives

Depending on the chosen method, different directives will be available.

To expand a directive branch, click once on the directive folder.

Additional directives may be created by highlighting the root (project name) so as to select it, and then by *right clicking* to bring up a context sensitive menu.

Add Directive is then chosen. The new directive will be added at the bottom of the tree.

- Another way is to select and *right click* on an existing directive to bring up a context sensitive menu, and then choosing **Insert Directive**. The new directive will be added above the currently selected directive.

2. Subdirectives

To **Add Subdirective**, first highlight a directive. To **Insert Subdirective**, highlight another subdirective.

3. Parameters

To **Add Parameter**, first highlight a subdirective.

Parameters are edited by *double clicking* on the desired parameter.

By default, parameters are preset to generally accepted values.

- Once all the desired parameters have been set, the user should click on **Save Settings** and then on **Run**.
- If simulation was successful, **2D Output** and **3D Output** will become bold.

4.2.3 Viewing output

The **3D Output** button becoming bold signifies that a simulation was run and completed properly. To view the simulation results, click the **3D Output** or **2D Output** buttons. The results are displayed by SibGraf.

- Clicking on 2D Output will bring up an empty 2D SibGraf window. Clicking on 3D Output will bring up a SibGraf Map window displaying a colour map of electrostatic potential .

1. SibGraf Map

- The map graph view settings are changed from the **View** menu.
- Clicking **Plot/Select...** brings up a list of variables that may be plotted.
- The first four buttons allow the user to highlight any X and Y cross section. This is accomplished with the cursor keys as well.
- The X, Y, as well as the Z value at the intersection of the two highlighted cross sections may be read from the SibGraf status bar.
- The second and third buttons from the right plot the selected cross sections in a separate SibGraf 2D window.
- The fourth button opens a SibGraf 3D window.

2. SibGraf 3D

- Clicking **Plot/Select...** brings up a list of variables that may be plotted.
- The first four buttons from the left allow the user to rotate the graph about

any axis.

- The next four buttons allow the user to highlight any X and Y cross section. This is accomplished with the cursor keys as well.
- The X, Y, as well as the Z value at the intersection of the two highlighted cross sections, may be read from the SibGraf status bar.
- The third last button draws a colour map of the displayed function.
- The last two buttons provide the ability to plot the selected cross sections in separate SibGraf 2D windows. This may be done repeatedly and for different functions; new cross sections will continue to be plotted in the same SibGraf 2D window. This is helpful in finding relations as well as getting a feel for parameters.

3. SibGraf 2D

- Click on **Curve** then **Add...**, and select the variables which will lie on the X and Y axis. Click on **Add** to add the curve to the graph.
- The first two buttons allow selecting different curves, the next two buttons move the marker along the selected curve. This may be done with the cursors as well.
- All curves may be **Curve/Copy**'d and **Curve/Paste**'d into existing Sibgraf 2D windows to facilitate comparison.
- *All graphs may be zoomed by using the mouse to draw a box.*
- After a successful run and display, one may return to **Project Settings**, change a value, re-**Save Settings** and re-**Run** the simulation. Clicking once again on the **3D Output** button, new cross-sectional graphs may be plotted for given functions with the old curves still present in the SibGraf 2D window (make sure you don't close it!). Each new cross-section will go into the proper old window; new Doping concentration cross sections will join the old Doping concentration curves. In this manner it is possible to precisely analyze the impact incurred from changed parameters and additional directives.

4.3 General Tips

- Pay attention to units in the project settings.
- Normally, the default models are sufficient. But to view junction breakdown, impact ionization must be turned on.
- Use the File/Print to copy graphics into Word or another editor. You may then select Post-Script or Windows Meta File formats for the output file.
- Add the **Batch Mode** parameter under **Basic->Numerical Solution Parameters**. Setting this parameter to zero will cause the calculations to stop after each iteration, giving the user a chance to analyze and graph the data before letting MicroTec proceed with further calculations by pressing the <Enter> key. By setting **Batch Mode** to one, the calculations are performed without stopping, and the output file is overridden after every I-V point is evaluated.

5. Device Simulation Directives and Parameters

5.1 Run Requirements

In order for a [SemSim](#) simulation to run successfully, several things are required:

5.1.1 Electrodes

There must be at least one electrode on the domain. It may be anywhere, and be any size. Electrodes may not overlap. As well, each electrode must have a unique **Electrode number**. The numbers are used to identifying the electrode when setting initial voltages and [ramping contacts](#). Each electrode should also have a distinguishing name (**Comment** parameter). The first letter of each name is used by SibGraf 2D to distinguish between the electrodes when plotting IV characteristics. See “Electrodes” on page 36 for more details.

5.1.2 IV Data

The IV Data directive must have at least one IV Data subdirective. The device must be biased in order for the 3D functions to be calculated. If more than one IV point are specified (Number of IV points to compute > 1) and [Batch Mode](#) is on, when the run is completed only the data for the last IV point remain. See “SibGraf 2D” on page 36 for more details.

5.1.3 Doping wells

The entire domain must be covered by a non-zero doping concentration. This may be achieved by a single, or a patchwork of doping wells. A non-zero concentration may be achieved even if the domain isn’t entirely covered by wells; the diffusion from the wells may be sufficient. Doping wells may overlap. See “Doping wells” on page 35 for more details.

5.2 Tips

5.2.1 Batch mode

Whenever on (1), all the calculations will proceed without stopping; the IV points will be calculated one after the other. When batch mode is turned off (0), the calculation will pause after each IV point. This gives the user a chance to click **3D Output**, and plot functions evaluated at the last computed IV point.

5.2.2 Doping wells

It must be noted that acceptor concentrations, N_a , are entered as negative numbers in MicroTec. A mobile hole leaves a negative ion. Similarly, donor concentrations, N_d , are entered as positive numbers. A free electron leaves a positive ion. N_a and N_d are specified in Analytical Doping Data/Analytical Doping Data/Doping concentration parameters. Inside the defined area the Doping concentration of a well is constant at the specified value. The concentration falls off as a Gaussian function outside the well. The characteristic length of the Gaussian is specified in Y characteristic length for the Y direction and X characteristic length for the X direction. A well of zero thickness still has a concentration gradient around it.

5.2.3 Axes

For manufacturing reasons positive Y is downward. The Z dimension, which is set in the **Basic/Mesh/Domain Z** parameter, is used as a multiplicative factor in current calculations and doesn’t figure anywhere else; doping wells and electrodes are automatically assumed to cover the entire Z domain. When setting domain sizes it helps to imagine the X-axis as

extending to the left, and the Y axis as extending down (if your monitor face was the domain, then the top left corner would be (0,0). X increases to the right, Y increases down)

5.2.4 Output

In order to improve output, the following parameters may be added and set:

Basic/Mesh/First Y mesh step size (0.003).

Basic/Mesh/Remesh (3).

These parameters improve the resolution and quality of output.

Basic/Numerical solution/Gummel iteration limit (300).

Basic/Numerical solution/Gummel residual to stop (0.003).

The last two parameters are used by the numerical method algorithms.

5.2.5 Ramping

IV Data/IV Data/Ramped electrode refers to the electrode on which a variable voltage will be applied. The initial voltage for all the contacts (electrodes) may be specified by setting the **Initial contact voltage #x** parameter, where x corresponds to the **Electrode number** parameter found under **Electrodes/[Ohmic electrode|Gate electrode|Schottkey electrode]/Electrode number**. When calculating IV characteristics, it is a good idea to add as many **Initial contact voltage** parameters as there are electrodes and set the proper values. The voltage on the **Ramped electrode** will start at **Initial contact voltage #x** and be incremented by **Voltage step size** for **Number of IV points to compute** points. To see the effects of bias on 3D functions, set the voltage of a contact to the desired value, set the number of IV points to compute to 1 and run the simulation.

5.2.6 SibGraf 3D

In order to display a 3D function, once a simulation has successfully run click the **3D Output** button. A SibGraf Map window appears. Select the desired functions from the **Plot/Select...** menu. See “SibGraf 3D” on page 32 for more details.

5.2.7 SibGraf Map

To display a map graph, click the **3D Output** button after a successful simulation run, or click the map button in Sibgraf 3D. See “SibGraf Map” on page 32 for more details.

5.2.8 SibGraf 2D

In order to display a 2D IV curve, following a successful run click the **2D Output** button. An empty SibGraf 2D window appears. From the **Curve** menu, click the **Add...** button. Select which variables will be plotted on which axis. Usually, voltage goes on the X axis, while current goes on the Y. Click **Add** to plot the curve, then **Close** to return to the SibGraf 2D window. The letters after “V” and “I” are the first letters in the electrode names.

There are two ways of displaying multiple curves. First, one could copy the **IV Data/IV Data** subdirective several times, changing parameters accordingly. For example, to see the effect of bulk voltage on threshold voltage in a MOSFET. Then **Add every odd family** to a SibGraf 2D window. The even families correspond to transconductance and output resistance curves. If there are 3 **IV Data/IV Data** subdirectives, there will be 6 families to choose from. Another way of plotting multiple curves is to **Curve/Copy** and **Curve/Paste** curves between windows. See “SibGraf 2D” on page 33 for more details.

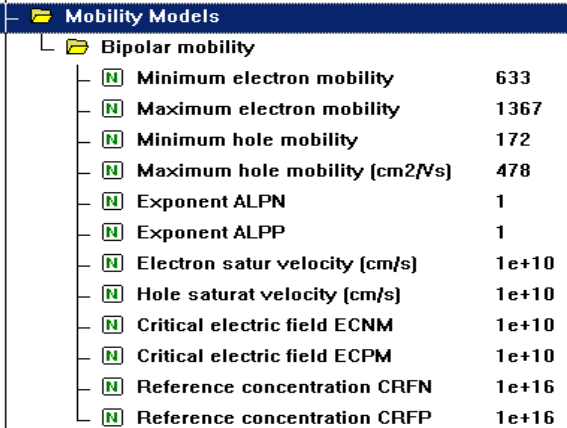
5.2.9 Electrodes

Extend domains to minimize the effects of electrodes (when analyzing photogeneration, for example); electron and hole concentrations fall near electrodes.

6. Building the p-n junction

The following procedure will detail the construction of a p-n junction. One will then be able to use this diode in a whole slew of problems by **Copying** this project and altering the parameters. For more explanations dealing with MicroTec specific question, refer to the Companion.

1. **Create** a new SemSim project under any name.
2. Switch to '**Project Settings**'; only three directives are present: **Basic**, **Electrodes** and **IV-data**.
3. Set a reasonable domain; if the problem states a specific area, then set the X and **Z domains** accordingly. The Y domain is set according to the following problem requirements: some problems deal with long p-n devices while others with short devices. For now, set the values for the X, Y and Z domains to 1, 3 and 1 respectively.
4. Add two **Analytical doping data/Analytical doping data** sub-directives. These will be two **doping wells**, one for donors and one for acceptors. Each well will create either the n-type or the p-type material. Name them accordingly in the **Comment** parameter. One well will extend from 0 to 1 left to right, and 0 to 1.5 top to bottom. The other will extend from 0 to 1 left to right, and 1.5 to 3 top to bottom. Set the **Doping concentration** to the values given in the problem. Remember that acceptor doping will be negative, because holes leave behind negative ions. If the problem states that the junction is abrupt, decrease the **y-characteristic length** in both wells from $0.07\mu\text{m}$ to about $0.0007\mu\text{m}$.
5. Add **Material Properties/Temperature and Bandgap/Temperature**. Notice that it is already set to 300K. This default room temperature is always included in the calculations; it is not necessary to include temperature if it is 300K.
6. Add two **Electrodes/Ohmic electrode** subdirectives. This is necessary for the simulation to run properly. Place one electrode on the bottom by setting **Electrode location** parameter to 2. Place the other electrode on the bottom. Make sure to give your electrodes different **Electrode numbers**, and different **Electrode names**.
7. Add the **Basic/Physical Models/Heavy Doping Effects** parameter, and set it to 0. This will cause the p-n junction to behave more like the perfect model described in the book.
8. If the mobilities μ_n or μ_p are given in the problem, add the **Mobility/Constant mobility** sub-directive. Set the parameters accordingly. Note that the default value for $\mu_n = 1000 \text{ cm}^2/\text{Vs}$ and $\mu_p = 500 \text{ cm}^2/\text{Vs}$. Constant mobility is not the default model used by MicroTec. The sub-directive must be added whenever constant mobility is required. The Einstein relation is used to translate between dispersion coefficients and mobility.
9. If holes and electrons have different mobilities on the n and p sides, the **Mobility Models/Bipolar mobility** subdirective must be added. The bipolar mobility model is shown in the manual. This model is more complicated than what is required by the book, and so the values must be set appropriately. If we assume $v_{\text{sat}, n}$, $v_{\text{sat}, p}$, E_{cmn} and E_{cmp} to be infinite, and set



Mobility Models	
Bipolar mobility	
Minimum electron mobility	633
Maximum electron mobility	1367
Minimum hole mobility	172
Maximum hole mobility (cm ² /Vs)	478
Exponent ALPN	1
Exponent ALPP	1
Electron satur velocity (cm/s)	1e+10
Hole saturat velocity (cm/s)	1e+10
Critical electric field E _{CMN}	1e+10
Critical electric field E _{CPM}	1e+10
Reference concentration CRFN	1e+16
Reference concentration CRFP	1e+16

Figure 1. Bipolar mobility model

$N_{\text{ref},n}, N_{\text{ref},p} = 10^{16}$ and $\alpha_n, \alpha_p = 1$, the equation is greatly simplified. Figure 1 shows the parameter declaration needed to achieve the following:

<u>p-side</u>	<u>n-side</u>
$\mu_p = 200 \text{ cm}^2/\text{V}\cdot\text{s}$	$\mu_n = 1300$
$\mu_n = 700$	$\mu_p = 450$

10. Lifetimes τ_n and τ_p are set by including the **Recombination parameters/SRH recombination parameters** sub-directive. As in the case of bipolar mobility, MicroTec's recombination model is more complex than the one used in the book. The manual shows the complete model. By assuming that $N_{\text{SRH},n}$ and $N_{\text{SRH},p}$ are infinite, the model reduces to $\tau_n = \tau_{n0}$ and $\tau_p = \tau_{p0}$. Figure 2 shows the parameter declaration needed to achieve $\tau_n = 0.1 \mu\text{s}$ and $\tau_p = 10 \mu\text{s}$.
11. In order to simulate a different semiconductor material, GaAs for example, it is necessary to set several values. **Material Properties/Temperature and Bandgap**, **Material Properties/Dielectric permittivity**, and constant mobility parameters. Figure 3 shows the necessary settings to simulate GaAs.
12. If **reverse IV characteristics** are required, the **Basic/Physical models/Impact ionization** parameter may be added. This will include the avalanche breakdown model.
13. Add an "IV-data" subdirective to "IV-data" directive. Even though IV characteristics might not be needed for a given problem, the subdirective is needed to run the simulation.
14. Add the **Basic/Numerical solution parameters/Batch mode** parameter if needed. "Save Settings" and "Run".

Recombination parameters	
SRH recombination parameters	
Electron life-time [s]	1e-07
Hole life-time [s]	1e-05
Concentration parameter NSRHN	1e+25
Concentration parameter NSRHP	1e+25

Figure 2. Shockley-Read-Hall model.

Material properties	
Temperature and Bandgap	
Bandgap width at 300 K [ev]	1.43
Dielectric permittivity	
Semicondctor dielectric permit.	13.2
Mobility Models	
Constant Mobility	
Electron mobility [cm ² /Vs]	8500
Hole mobility [cm ² /Vs]	400

Figure 3. Simulating GaAs.

Index

Symbols

- *.dbf 31
- *.mdx 31

Numerics

- 2D Graphs 36
- 2D Output 32, 33
- 3D Graphs 36
- 3D Output 32

A

- Add Curve 33, 36
- Add Directive 32
- Add Parameter 32
- Add Project 31
- Add Subdirective 32
- Axes 35

B

- Batch Mode 31, 33, 35

C

- Copy Project 31
- Cross Sections 33

D

- Directives 32
- Domains 35, 36
- Doping Wells 35

E

- Electrodes 35, 36, 37

I

- Insert Directive 32
- Insert Subdirective 32
- IV Data 35

M

- Map Graph 32, 36
- MergIC 31
- Methods 31
- MicroTec Tips 33, 35

Multiple plots 33, 36

N

New project 31

O

Ohmic electrode 36

Output 36

P

Parameters 32

Project selection/creation screen 31

R

Ramping 36

S

Save Settings 32

SemSim 31

SibGraf 2D 33, 36

SibGraf 3D 32, 36

SibGraf Map 32, 36

SiDif 31

Subdirectives 32

U

Update 31

List of Figures

Figure 5.4.1	Arsenic concentration profiles at different implant energies.	9
Figure 5.4.2	Arsenic concentration profiles at different implant doses.	9
Figure 5.5.1	Boron concentration profile.	10
Figure 5.6.1	Logarithm of net doping concentration for different annealing times.	11
Figure 5.6.2	Logarithm of net doping concentration for different P surface concentrations.	11
Figure 5.9.1	Electrostatic and Fermi potential.	12
Figure 5.6.3	Logarithm of net doping concentration for different annealing temperatures.	12
Figure 5.10.1	Electric field. Annotation lines mark the relative locations of x_{n0} and x_{p0} . Mobile carrier effects are clearly visible.	13
Figure 5.10.2	The effects of doping on peak electric field and spillover.	13
Figure 5.12.2	IV characteristic plot.	14
Figure 5.12.1	Electric field under 0 V bias.	14
Figure 5.13.1	Close-up of the electric field. Annotation lines mark x_{n0} and x_{p0}	16
Figure 5.13.2	Logarithm of excess carrier concentrations throughout transition region at 0 V and 0.5 V forward bias. Annotation lines mark x_{p0} and x_{n0}	16
Figure 5.13.3	Logarithm of electron and hole concentrations in a symmetrically doped GaAs junction under 0 V and 0.5 V forward bias.	16
Figure 5.14.1	Electrostatic potential used to find V_0	17
Figure 5.14.2	Reverse IV with breakdown.	17
Figure 5.14.3	Electric field at different biases.	17
Figure 5.14.4	EHP generation rates at different reverse biases.	17
Figure 5.14.5	Avalanche breakdown for different N_d	18
Figure 5.16.1	Equilibrium band diagram.	19
Figure 5.15.1	Changes in peak electric field E_0 due to variations in N_a	19
Figure 5.15.2	Changes in peak electric field E_0 due to variations in N_d	19
Figure 5.19.1	Electrostatic potential under 0 V bias for the long diode.	20
Figure 5.19.4	Current densities for long diode.	21
Figure 5.19.2	Under 0 V bias, depletion region width ~ 0.95 mm for yellow curve. Long diode. 21	
Figure 5.19.3	Logarithm of electron concentration on the p-side under 0.5 V forward bias. Long diode.	21
Figure 5.19.6	Logarithm of electron and doping concentrations on the p side under 0.5 V forward bias for the long diode.	22
Figure 5.19.7	Logarithm of electron and doping concentrations on the p side under 0.7 V forward bias for the long diode.	22
Figure 5.19.5	IV characteristic for long diode.	22
Figure 5.19.9	Hole concentration under 0.5 V forward bias for the long diode.	23
Figure 5.19.10	Electric field under 0.5 V forward bias for the long diode.	23
Figure 5.19.8	Electron concentration under 0.5 V forward bias for the long diode.	23
Figure 5.19.12	Electric field for short diode.	24
Figure 5.19.11	Electrostatic potential under 0 V bias for the short diode.	24
Figure 5.19.15	Electric field under 0.5 V forward bias.	25
Figure 5.19.16	IV characteristic for short diode.	25
Figure 5.19.13	Electron concentration under 0.5 V forward bias.	25

Figure 5.19.14	Hole concentration under 0.5 V forward bias	25
Figure 5.19.19	Current densities for short diode.	26
Figure 5.19.20	Logarithm of current densities for short diode.	26
Figure 5.19.17	Logarithm of electron and doping concentrations on the p side under 0.5 V forward bias for the short diode.	26
Figure 5.19.18	Logarithm of electron and doping concentrations on the p side under 0.7 V forward bias for the short diode.	26
Figure 5.19.21	Logarithm of electron and hole concentrations near transition region.	27
Figure 5.25.1	Reverse IV characteristic. For different donor concentrations with and without impact ionization.	29
Figure 5.25.3	Logarithmic plot of the EHP generation rate.	29
Figure 5.25.2	Transition region width is clearly visible in electric field diagrams.	29
Figure 1.	Bipolar mobility model	37
Figure 2.	Shockley-Read-Hall model.	38
Figure 3.	Simulating GaAs.	38